

1  
2  
3  
4  
5  
6  
7  
8  
9  
10  
11  
12  
13  
14  
15  
16  
17  
18  
19  
20  
21  
22  
23  
24  
25  
26  
27

Manuscript

**Proteomics of Extracellular Vesicles Produced by *Granulicatella***

**Species that cause Infective Endocarditis**

Sarah A Alkandari<sup>1</sup>, Radhika G Bhardwaj<sup>1</sup>, Arjuna Ellepola, and Maribasappa  
Karched<sup>1\*</sup>

<sup>1</sup>Oral Microbiology Research Laboratory, Department of Bioclinical Sciences, Faculty  
of Dentistry, Health Sciences Center, Kuwait University, Kuwait.

**\*Corresponding author**

Maribasappa Karched  
Oral Microbiology Research Laboratory  
Department of Bioclinical Sciences  
Faculty of Dentistry  
Kuwait University  
PO Box 24923  
Safat 13110  
Kuwait  
Tel: +965-24636643  
Email: [mkarched@hsc.edu.kw](mailto:mkarched@hsc.edu.kw)

28

## 29 **Abstract**

30           When oral bacteria accidentally enter the bloodstream due to transient tissue  
31 damage during dental procedures, they have the potential to attach to the endocardium  
32 or an equivalent surface of an indwelling prosthesis and cause infection. Many bacterial  
33 species produce extracellular vesicles (EVs) as part of normal physiology, but also use  
34 it as a virulence strategy. In this study, it was hypothesized that *Granulicatella* species  
35 produce EVs that possibly help them in virulence. Therefore, the objectives were to  
36 isolate and characterize EVs produced by these species and to investigate their immune-  
37 stimulatory effects. The reference strains *G. adiacens* CCUG 27809 and *G. elegans*  
38 CCUG 38949 were cultured on chocolate blood agar for 2 days. From subsequent broth  
39 cultures, the EVs were isolated using differential centrifugation and filtration protocol  
40 and then observed using scanning electron microscopy. Proteins in the vesicle  
41 preparations were identified by nano LC-ESI-MS/MS. The EVs proteomes were  
42 analyzed and characterized using different bioinformatics tools. The immune-  
43 stimulatory effect of the EVs was studied via ELISA quantification of IL-8, IL-1 $\beta$  and  
44 CCL5, major proinflammatory cytokines, produced from stimulated human PBMCs. It  
45 was revealed that both *G. adiacens* and *G. elegans* produced EVs, ranging in diameter  
46 from 30 to 250 nm. Overall, *G. adiacens* EVs contained 160 proteins, and *G. elegans*  
47 EVs contained 107 proteins. Both proteomes consist of several ribosomal proteins,  
48 DNA associated proteins, binding proteins, and metabolic enzymes. It was also shown  
49 that these EVs carry putative virulence factors including moonlighting proteins. These  
50 EVs were able to induce the production of IL-8, IL-1 $\beta$  and CCL5 from human PBMCs.  
51 The diversity in EVs content indicates that these vesicles could have possible roles in

52 bacterial survival, invasion, host immune modulation as well as infection. Further  
53 functional characterization of the *Granulicatella* EVs may provide new insights into  
54 virulence mechanisms of these important but less studied oral bacterial species.

55

## 56 **Introduction**

57 *Granulicatella* species, formerly known as nutritionally variant streptococci  
58 based on their characteristic dependence on pyridoxal or cysteine supplementation for  
59 their growth in standard media [1], are catalase and oxidase negative, non-motile, non-  
60 spore-forming, facultatively anaerobic Gram-positive cocci [2, 3]. They are part of the  
61 normal oral flora [4], but cause serious infections such as infective endocarditis. The  
62 genus *Granulicatella* consists of 3 species: *Granulicatella adiacens*, *Granulicatella*  
63 *elegans* and *Granulicatella balaenopterae* [3]. The species *G. balaenopterae* has not  
64 been isolated from human samples, whereas both *G. adiacens* and *G. elegans* have been  
65 reported from IE cases [5, 6]. In addition, these oral commensal cocci have been  
66 associated with endodontic infections [7, 8], dental caries [9], and periodontitis [8, 10]  
67 via DNA-based studies. Although this association does not substantiate the role of  
68 *Granulicatella* species in dental diseases, the fact that these species are causative agents  
69 in infective endocarditis implies that they might exert similar pathogenic potential also  
70 in the oral cavity.

71 Many bacterial species routinely produce extracellular vesicles (EVs) during  
72 normal growth [11]. Gram-negative bacteria are commonly found to produce such  
73 vesicles, which are derived from blebbing of the outer membrane and thus are called  
74 outer membrane vesicles (OMVs) [11]. Generally, these OMVs contain outer  
75 membrane proteins, lipopolysaccharides, glycerophospholipids in addition to enclosed

76 periplasmic components and bacterial nucleic acids [11-13]. The study of the EVs was  
77 initially limited to Gram-negative bacteria, as it was thought that the rigidity of the  
78 Gram-positive cell wall, which is rich in peptidoglycans, would not allow vesicle  
79 blebbing [11]. However, the production of EVs was also observed in some Gram-  
80 positive bacteria [14-17]. Current studies [18-20] showed that the activity of cell wall-  
81 degrading enzymes, which weaken the peptidoglycan layer and thus facilitate the  
82 release of Gram-positive EVs, could probably explain such phenomena in Gram-  
83 positive bacteria. Similar to Gram-negative OMVs, these EVs contain proteins, lipids,  
84 enzymes, toxins and bacterial nucleic acids [20]. However, Gram-positive EVs can still  
85 be distinguished from OMVs as the former lack lipopolysaccharide and enclosed  
86 periplasmic components [20].

87         Several studies [13, 14, 18] showed that bacteria exploit vesicle production as  
88 a virulence strategy. Bacterial components, including virulence factors, are packed in  
89 the vesicles and delivered to the host cells and tissues. The vesicle-derived virulence  
90 factors play an important role in bacterial pathogenicity, e.g., by eliciting an  
91 inflammatory response, manipulating the host's immunity, eliminating the competing  
92 commensal microorganisms, relieving internal stress, mediating biofilm formation, and  
93 acting as decoys absorbing and blocking cell wall-lytic compounds and membrane-  
94 disrupting antimicrobial peptides produced by other commensals and host innate  
95 immune cells [13, 14, 18].

96         Protein secretion in *Granulicatella* species has been studied [21], but vesicle  
97 production in these species has not been investigated yet. In this study, it was  
98 hypothesized that *Granulicatella* species produce EVs that possibly play a role in the  
99 pathogenesis of *Granulicatella* infections.

## 100 **Materials and methods**

### 101 **Bacterial strains and culture conditions**

102 The reference strains *G. adiacens* CCUG 27809 and *G. elegans* CCUG 38949  
103 were cultured on chocolate blood agar (CBA) with 0.001% pyridoxal hydrochloride at  
104 37 °C and in 5% CO<sub>2</sub> in air for 2 days. A loop-full of colonies from the CBA plates  
105 was inoculated into brucella broth supplemented with 0.001% pyridoxal hydrochloride  
106 and incubated as above for 2 days.

107

### 108 **Isolation of EVs**

109 The EVs were isolated using a previously described centrifugation and filtration  
110 protocol [22], with slight modifications. Briefly, for pelleting the bacteria, the broth  
111 culture was centrifuged at 5000 × g at room temperature for 10 minutes (Centrifuge  
112 5430 R, Eppendorf AG, Germany). For removing any remnants of intact bacterial cells,  
113 the supernatant was filtered through a 0.22 µm sterile syringe filter (Millipore,  
114 Germany). The filtrate was then re-centrifuged at 125000 × g at 4° C for 3 hours  
115 (Optima™ L-XP ultracentrifuge, Beckman, USA). The obtained pellet was suspended  
116 in 300 µl sterile phosphate-buffered saline (PBS). The EVs samples were stored at -20°  
117 C until used.

118

### 119 **Preparation of whole cell protein (WCP)**

120 A loop full of colonies from the CBA plates was suspended in 2 ml sterile PBS. The  
121 bacterial suspension was centrifuged at 5000 ×g at room temperature for 5 minutes  
122 (Centrifuge 5430 R, Eppendorf AG, Germany). Then, after discarding the supernatant,  
123 the pellet was washed with 2 ml sterile PBS. The bacterial whole cell protein (WCP)  
124 was obtained by ultra-sonicating bacterial cells at 40 pulse rate on ice for 8 cycles (1

125 minute sonication followed by 1 minute rest per cycle) (Omni Sonic Ruptor 4000, Omni  
126 International, USA) followed by centrifugation at 7000 ×g at 4° C for 10 minutes  
127 (Centrifuge 5430 R, Eppendorf AG, Germany). The resulting supernatant was used as  
128 the WCP sample and stored at -20° C until used.

129

## 130 **Characterization of EVs**

### 131 **Scanning electron microscopy (SEM)**

132 The obtained vesicle preparations were suspended in sterile PBS containing 3%  
133 glutaraldehyde for 2 hours on a rotator and then kept in a refrigerator overnight. For  
134 staining, the vesicle samples were incubated in 1% osmium tetroxide for 2 hours. For  
135 dehydration, the samples were kept in increasing concentrations of acetone from 30 to  
136 100%, 10 minutes in each, on a rotator. The samples were then placed in a critical point  
137 dryer for complete drying, mounted on stubs with carbon double adhesive tape and  
138 finally coated with gold and stored in a desiccator until observation. The samples were  
139 observed on Zeiss Leo Supra 50VP field emission scanning electron microscope  
140 (Carl Zeiss, Germany). For comparison, SEM analysis of bacterial whole cells was also  
141 performed using the same previous biological sample preparation protocol.

142

### 143 **Determination of protein concentration and SDS-PAGE**

144 Protein concentrations in the EVs and WCP samples were determined by Quick Start™  
145 Bradford protein microplate standard assay (Bio-Rad, USA). For protein separation, the  
146 samples were subjected to sodium dodecyl sulfate-polyacrylamide gel electrophoresis  
147 (SDS-PAGE) using the mini-PROTEAN II cell electrophoresis system (Bio-Rad,  
148 USA). The proteins were denatured in 2× loading buffer at 100°C for 5 minutes,  
149 followed by centrifugation at 5000 ×g for 5 minutes. 20 µl of proteins loaded in each

150 well of the gel were separated on 12% SDS-PAGE at a constant 120 V. After the run  
151 was completed, protein bands were detected using silver stain. Gel images were  
152 visualized in G: Box Imaging System (Syngene, India). Protein banding patterns and  
153 molecular weights of the bands were determined using GeneSys tools software

154

### 155 **Identification of EVs proteins by Nano-LC-ESI-MS/MS**

156 For the identification of EVs proteins, mass spectrometry was performed by  
157 Proteome Factory (Proteome Factory AG, Berlin, Germany) using nano-liquid  
158 chromatography-electrospray ionization-tandem mass spectrometry (nano-LC-ESI-  
159 MS/MS). After pooling replicate samples from EVs preparations, 400 ng proteins were  
160 reduced, alkylated and digested by trypsin (Promega, Mannheim, Germany). Then, the  
161 resulting peptides were subjected to the nanoLC-ESI-MS/MS. 1% acetonitrile/0.5%  
162 formic acid was used as eluent for 5 minutes to trap and desalt the peptides on the  
163 enrichment column (Zorbax SB C18, 0.3 × 5 mm, Agilent). An acetonitrile/0.1% formic  
164 acid gradient from 5% to 40% acetonitrile was then used within 120 minutes to separate  
165 the peptides on a Zorbax 300 SB C18, 75 µm x 150 mm column (Agilent). The mass  
166 spectrometer automatically recorded the mass spectra according to the manufacturer's  
167 settings. Protein identification was made using the Mascot search engine (Matrix  
168 Science, London, England) and the National Center for Biotechnology Information  
169 non-redundant (NCBI-nr) protein database, version 20151202, (NCBI, Bethesda,  
170 USA). Ion charge in search parameters for ions from ESI-MS/MS data acquisition was  
171 set to "1+, 2+ or 3+" according to the instrument's and method's standard charge state  
172 distribution. The search parameters were: Fixed modifications: Carbamidomethyl (C);  
173 variable modifications: Deamidated (NQ), Oxidation (M); Peptide Mass Tolerance: ±  
174 5 ppm; Fragment Mass Tolerance: ± 0.6 Da; Missed Cleavages: 2. The inclusion

175 criterion was: peptides that match with a score of 20 or above. Mass spectrometry data,  
176 with the project accession number PXD015630, has been deposited at PRIDE archive  
177 (<https://www.ebi.ac.uk/pride/archive/>) repository. The data files can be accessed with  
178 the username **reviewer51332@ebi.ac.uk** and the password **k0SBY6YK**.

179

## 180 **Bioinformatic analysis**

181 Protein sequences from the liquid chromatography-mass spectrometer (LC-MS)  
182 analysis of the EVs proteomes were analyzed by an *in silico* 2-dimensional  
183 electrophoresis (2-DE) tool. For this, the software JVirGel, version 2.0  
184 (<http://www.jvirgel.de/index.html>), was used to obtain a theoretical (2-DE) image of  
185 the EVs proteins [23]. The subcellular localization of the EVs proteins detected with  
186 LC-MS/MS was predicted using the PSORTb tool, version 3.0.2  
187 (<https://www.psорт.org/psорт/>) [24]. To determine if any of the secreted proteins are  
188 packed into the vesicles, the prediction tool SignalP, version 5.0  
189 (<http://www.cbs.dtu.dk/services/SignalP/abstract.php>), was utilized to predict proteins  
190 secreted via the general Secretion route (Sec-pathway) [25]. In addition to that, the  
191 prediction tool TatP (<http://www.cbs.dtu.dk/services/TatP/>), was used to predict  
192 proteins secreted via the Twin-arginine translocation pathway (Tat-pathway) [26]. To  
193 identify lipoproteins, lipoboxes were searched using the prediction tools LipoP  
194 (<http://www.cbs.dtu.dk/services/LipoP/>) and PRED-LIPO  
195 (<http://bioinformatics.biol.uoa.gr/PRED-LIPO/input.jsp>) [27].

196

## 197 **Function prediction analysis**



198 Proteins with multiple functions, known as “moonlighting proteins”, were  
199 identified using the prediction tool moonprot, version 2.0  
200 (<http://www.moonlightingproteins.org/>) [28], and searching the database Multitask  
201 ProtDB (<http://wallace.uab.es/multitaskII/>) [29]. Gene Ontology (GO) analysis of the  
202 EVs proteomes was performed using the amino acid FASTA sequences of *G. adiacens*  
203 and *G. elegans*. For this, GO annotations were analyzed and plotted using the tools  
204 Blast2GO (<https://www.blast2go.com/>) [30], and WEGO, version 2.0  
205 (<http://wego.genomics.org.cn/>) [31]. The EVs proteins were grouped based on  
206 functional association networks using the tool STRING (<https://string-db.org/>) [32].  
207 Minimum interaction scores were set at a strong confidence level of 0.7. The EVs  
208 proteins were also grouped based on different biological pathways. For this, all protein  
209 sequences from *G. adiacens* and *G. elegans* EVs proteomes were analyzed by the Kyoto  
210 Encyclopedia of Genes and Genome (KEGG)  
211 (<https://www.genome.jp/kegg/pathway.html>) pathway analysis tool using the genus  
212 “streptococcus” as reference [33].

### 213 **Prediction of virulence factors in the EVs proteomes**

214 To predict virulence proteins in the EVs proteomes, the tool VirulentPred  
215 (<http://203.92.44.117/virulent/>) [34], along with the Virulence Factor Data Base  
216 (VFDB; <http://www.mgc.ac.cn/VFs/>) were used. Proteins predicted to be virulent by  
217 the previous tools were manually searched in the literature for experimental evidence  
218 on their virulence properties.

### 219 **Cytokine induction of human PBMCs by EVs**

#### 220 **Isolation of human PBMCs**

221 PBMCs from the blood of a healthy human volunteer were isolated using Ficoll-  
222 Paque density gradient centrifugation method [35]. After obtaining written informed  
223 consent from the donor, blood was collected by venipuncture into vacutainer heparin  
224 tubes (3 ml per tube). The blood was then carefully layered onto 3.5 ml Ficoll-Paque  
225 media solution (GE Healthcare, USA) in a sterile centrifugation tube. For separating  
226 mononuclear cells, the tubes were centrifuged at  $3400 \times g$  at room temperature with the  
227 brakes off for 10 minutes. The layer of PBMCs, the buffy coat layer, was then  
228 transferred to another sterile centrifugation tube. The cell isolate was washed twice by  
229 resuspending it in 5 ml RPMI medium followed by centrifugation at 2000 rpm at room  
230 temperature with the brakes on for 5 minutes. The supernatant was discarded, and the  
231 cell pellet was finally resuspended in 1 ml RPMI medium supplemented with 10% heat-  
232 inactivated fetal bovine serum and 2% Gibco™ 100× antibiotic-antimycotic solution.  
233 Cell concentration in the PBMCs sample was estimated by loading 10 µl aliquot on a  
234 hemocytometer under 400× magnification.

235

### 236 **Stimulation of human PBMCs with EVs and WCP**

237 Isolated human PBMCs were stimulated with different concentrations (10, 25, 50,  
238 and 100 µg/ml) of *G. adiacens* EVs, *G. adiacens* WCP, *G. elegans* EVs, and *G. elegans*  
239 WCP for 24 hours. For this, in a 24-well plate, 480 µl supplemented RPMI medium  
240 containing PBMCs ( $10^6$  cells per ml) was added to each well and stimulated with 20 µl  
241 of bacterial EVs or WCP. The plate was incubated at 37 °C and in 5% CO<sub>2</sub> in air for 24  
242 hours. Well with 20 µl sterile PBS and 480 µl RPMI medium containing PBMCs was  
243 used as negative control.

### 244 **Quantitative determination of selected cytokines**

245 The quantitative sandwich enzyme-linked immunosorbent assay (ELISA)  
246 technique was used to quantify the production of the human cytokines IL-8, IL-1 $\beta$ , and  
247 CCL5 (RANTES) from the stimulated PBMCs. For this, ELISA immunoassay kits  
248 (Quantikine<sup>®</sup> ELISA R&D systems, Bio-Techne, USA) were used according to the  
249 manufacturer's instructions. Briefly, standards, samples, and controls were added to the  
250 wells of a 96-well microplate pre-coated with a monoclonal antibody specific for the  
251 cytokine of interest. To allow the specific cytokine in the sample to be bound by the  
252 specific immobilized antibody, the plate was incubated at room temperature for 2 hours.  
253 To remove any unbound substances, the wells were washed with wash buffer using  
254 ImmunoWash<sup>™</sup> 1575 microplate washer (Bio-Rad, USA). Then, an enzyme-linked  
255 polyclonal antibody for the specific cytokine was added to each well. After an  
256 incubation period of one hour at room temperature, the wells were washed again with  
257 wash buffer to remove any unbound antibody-enzyme reagent. A substrate solution was  
258 then added to each well, and the microplate was incubated at room temperature for 20-  
259 30 minutes while being protected from light. To terminate the colorful enzyme-  
260 substrate reaction, a stop solution was added to each well. Finally, iMark<sup>™</sup> microplate  
261 reader was used to measure the intensity of the color developed.

262

## 263 **Statistical analysis**

264 All experiments were repeated twice. Statistical Package for Social Sciences  
265 Software (SPSS), version 25, was used for data analysis. Descriptive statistics were  
266 presented using mean  $\pm$  standard deviation (SD). Independent-samples T test and Mann  
267 Whitney U test were used to analyze differences between groups. A critical probability  
268 value (P value) of  $< 0.05$  was used as the cut-off level for statistical significance.

269

## 270 **Ethical considerations**

271 This study was approved by the ethical committee of the Health Sciences Center,  
272 Kuwait University (DR/EC/3413), and has been carried out in full accordance with the  
273 World Medical Association Declaration of Helsinki. The blood donor received written  
274 information about the nature and purposes of the study and a written informed consent  
275 was obtained upon his/her approval to participate.

276

## 277 **Results and discussion**

### 278 **Isolation of EVs**

279 It was revealed by the current study that both *G. adiacens* and *G. elegans*  
280 produce EVs. Vesicles of varying sizes, ranging from 30 to 250 nm in diameter, were  
281 seen in the electron micrographs. This nano-scale range size was consistent with other  
282 bacterial EVs [14, 16]. For comparison, images of bacterial whole cells (Figs 1A and  
283 2A) and the vesicle preparations (Figs 1B and 2B) were captured at the same  
284 magnification of  $\times 10000$ . Vesicle shape and size could be visualized better at a higher  
285 magnification of  $\times 40000$  (Figs 1C and 2C).

286

287 **Fig 1. SEM images of *G. adiacens* whole cells and the EVs preparation.** SEM images  
288 of bacterial whole cells (A) and the EVs preparation (B) captured at the magnification  
289  $\times 10000$ . (C) SEM images of the EVs acquired at  $\times 40000$ .

290 **Fig 2. SEM images of *G. elegans* whole cells and the EVs preparation.** SEM  
291 images of bacterial whole cells (A) and the EVs preparation (B) captured at the  
292 magnification  $\times 10000$ . (C) SEM images of the EVs acquired at  $\times 40000$ .

## 293 **Characterization of EVs**

### 294 **Determination of protein concentration and SDS-PAGE**

295 Protein concentrations in the EVs samples from both *G. adiacens* and *G.*  
296 *elegans*, 1337 µg/ml and 1339 µg/ml respectively, were much lower compared to their  
297 respective WCP samples, 3102 µg/ml and 3388 µg/ml respectively. Consistently, SDS-  
298 PAGE analysis revealed that the EVs preparations from both *G. adiacens* and *G.*  
299 *elegans* showed much fewer bands on gel than their respective WCP preparations (Fig  
300 3A).

301

302 **Figure 3. Analysis of the proteome of *G. adiacens* and *G. elegans* EVs.** (A) SDS-  
303 PAGE gel showing protein bands from EVs and WCP preparations. (B) and (C)  
304 Protein sequences from LC-MS analysis of the vesicle proteome analyzed by an *in*  
305 *silico* 2-DE tool.

306

### 307 **Identification of EVs proteins by NanoLC-ESI-MS/MS**

308 In total, 160 and 107 proteins detected by NanoLC-ESI-MS/MS in EVs  
309 preparations of *G. adiacens* and *G. elegans* respectively, were analyzed and defined as  
310 the EVs proteomes in the present study (Suppl. Table 1 and 2). These numbers were  
311 within the range of proteins identified in previous analyses of other bacterial vesicle  
312 proteomes [14, 16, 17].

313

### 314 **Bioinformatic analysis**

315 *In silico* 2-DE analysis of the EVs proteomes showed that the molecular mass of  
316 the proteins ranged between 14.9 kDa and 125.7 kDa for *G. adiacens* (Fig 3B), and  
317 between 20 kDa and 195 kDa for *G. elegans* (Fig 3C). The proteome of *G. adiacens*

318 EVs formed a distinct cluster with respect to predicted isoelectric point (pI) values in  
319 the range of 4.0 and 6.4 (Fig 3B). In the case of *G. elegans* EVs, the proteins seemed to  
320 be more dispersed in the pI range, showing some clustering of proteins in the pI range  
321 4.0 to 5.6 (Fig 3C).

322 According to the PSORTb subcellular localization prediction tool analysis, *G.*  
323 *adiacens* EVs proteome was predicted to contain 113 cytoplasmic proteins, 27  
324 cytoplasmic membrane proteins, and 4 cell-wall anchored proteins; whereas the  
325 localization of 16 proteins could not be predicted. Similarly, *G. elegans* EVs proteome  
326 was predicted to contain 67 cytoplasmic proteins, 20 cytoplasmic membrane proteins,  
327 2 cell-wall anchored proteins and 18 proteins of unknown localization. As predicted in  
328 this study, the majority of EVs proteins were cytoplasmic in both *G. adiacens* and *G.*  
329 *elegans* proteomes (71% and 67% respectively). Cytoplasmic proteins located in other  
330 bacterial vesicles have been reported in several earlier studies [36, 38]. Existing  
331 evidence suggests that the enormous location of cytoplasmic proteins into vesicles is  
332 due to specific sorting mechanisms, and not due to lysis of dead cells [39]. Importantly,  
333 cytoplasmic proteins released as part of vesicles are known to function as adhesins,  
334 contribute to biofilm matrix formation, and help bacteria in evading the immune system  
335 [40].

336

337 As predicted in our study by the SignalP and TatP tools, secretory proteins were  
338 packed into the EVs of both *Granulicatella* species. According to the SignalP prediction  
339 tool, 38 proteins of *G. adiacens* EVs proteome were found to contain a signal sequence,

340 while 18 of the *G. elegans* EVs proteins were predicted to contain a signal sequence.  
341 This suggests that such proteins are probably secreted via the Sec- pathway. The TatP  
342 prediction tool showed that 12 proteins of the *G. adiacens* EVs proteome and 13  
343 proteins of the *G. elegans* EVs proteome contained TatP signal sequence, suggesting  
344 the Tat pathway for their secretion. Both the Sec and Tat pathways are major pathways  
345 that exist in bacteria for proteins secretion across the cytoplasmic membrane [41, 42].  
346 The former pathway is well known to translocate proteins in their unfolded  
347 conformation, while the latter catalyzes the secretion of proteins that fold before their  
348 translocation [42]. It is well-established that protein secretion is an essential strategy in  
349 the pathogenesis of bacterial infections [41]. “Secreted proteins can play many roles in  
350 promoting bacterial virulence, from enhancing attachment to eukaryotic cells, to  
351 scavenging resources in an environmental niche, to directly intoxicating target cells and  
352 disrupting their functions” [41]. Lipoprotein prediction tools (Pred-Lipo, LipoP)  
353 revealed that there were 23 lipoproteins in the *G. adiacens* EVs proteome, and 10  
354 lipoproteins in the *G. elegans* EVs proteome.

355

## 356 **Function prediction analysis**

357 The present study showed that EVs from both *Granulicatella* species carry  
358 proteins predicted to exhibit multitasking capabilities. Table 1 lists the 12 proteins from  
359 the *G. adiacens* EVs proteome and the 7 proteins from the *G. elegans* EVs proteome,  
360 respectively, that were identified as “moonlighting proteins”. Major proteins predicted  
361 as multifunctional proteins were ribosomal proteins and molecular chaperones.  
362 Additionally, a glycolytic enzyme, glyceraldehyde-3-phosphate-dehydrogenase, and a  
363 few putative virulent proteins such as NADH oxidase and thioredoxin were also  
364 identified. Such multifunctional bacterial proteins were found to play a role in the

365 virulence of several other human pathogenic bacteria; e.g., *Staphylococcus*  
366 *aureus*, *Streptococcus pyogenes*, *Streptococcus pneumoniae*, *Helicobacter pylori*,  
367 and *Mycobacterium tuberculosis* [43-45].

368

369 **Table 1. Predicted moonlighting proteins from *G. adiacens* and *G. elegans* EVs**  
370 **proteome.**

GI Number	Protein
<b><i>G. adiacens</i></b>	
gi 491802570	Serine protease
gi 491797953	Molecular chaperone DnaK
gi 491800441	Superoxide dismutase
gi 491800797	Glyceraldehyde-3-phosphate dehydrogenase
gi 491800365	NADH oxidase
gi 748591028	30S ribosomal protein S20
gi 491801600	50S ribosomal protein L7/L12
gi 491802592	30S ribosomal protein S6
gi 259036192	Thioredoxin
gi 491801148	Elongation factor Tu
gi 491801605	50S ribosomal protein L10
gi 259035990	Phosphoglycerate kinase
<b><i>G. elegans</i></b>	
gi 491797953	Molecular chaperone DnaK
gi 491800797	Glyceraldehyde-3-phosphate dehydrogenase
gi 491800365	NADH oxidase
gi 491799730	Short-chain dehydrogenase
gi 491801600	50S ribosomal protein L7/L12
gi 491802592	30S ribosomal protein S6
gi 491801148	Elongation factor Tu

371

372 Fig 4 summarizes the Gene Ontology analysis of the EVs proteomes. Overall,  
373 112 of the *G. adiacens* sequences and 108 of the *G. elegans* sequences were assigned  
374 with GO annotation. For *G. adiacens* and *G. elegans*, the proteins were divided into 3  
375 groups based on GO terms: 90 and 61 proteins in “biological process” group, 28  
376 proteins each in the “cellular component” group, and 104 and 70 proteins in the



377 “molecular function” group, respectively. According to the Gene Ontology analysis  
378 conducted in the present study, most proteins in both *G. adiacens* EVs and *G. elegans*  
379 EVs proteomes were predicted to be involved in molecular functions, particularly  
380 catalytic and binding functions, followed by biological processes, mainly metabolic and  
381 cellular processes. It is possible that these species might utilize nutrients in the  
382 environment by using the metabolism-mediator proteins in the EVs [46]. Only 28  
383 proteins in both proteomes were annotated for cellular components. Similar to other  
384 bacterial EVs, *G. adiacens* and *G. elegans* EVs contained several ribosomal proteins,  
385 DNA associated proteins, binding proteins, and metabolic enzymes, indicating that  
386 bacterial EVs might facilitate the transfer of functional proteins [14, 18].

387

388 **Fig 4. Gene Ontology analysis of the proteomes of *G. adiacens* and *G. elegans***

389 **EVs preparations.** Gene ontology annotation was achieved using Blast2GO and an  
390 online software “WEGO”. Protein sequences were grouped into 3 categories based on  
391 their properties and functions.

392

393 Figures 5 and 6 demonstrate the STRING functional protein association network  
394 analysis of *G. adiacens* EVs proteome and *G. elegans* EVs proteome, respectively. As  
395 demonstrated in our study, both *G. adiacens* and *G. elegans* EVs proteomes formed  
396 three distinct protein groups based on their functional associations. These groups were  
397 carbohydrate metabolism, ribosomal proteins, and heat shock proteins/chaperones.  
398 Components of the carbohydrate metabolism network were: glyceraldehyde-3-  
399 phosphate dehydrogenase, phosphoenolpyruvate-protein phosphotransferase, glucose-  
400 6-phosphate isomerase, phosphoglycerate kinase, Pyruvate kinase, ATP-dependent 6-  
401 phosphofructokinase, transketolase, pyruvate dehydrogenase E1 component, and

402 dihydrolipoamide acetyltransferase component of pyruvate dehydrogenase complex.  
403 The ribosomal protein group consisted mainly of the secreted ribosomal proteins: 30S  
404 ribosomal protein S20, 50S ribosomal protein L10, 30S ribosomal protein S5, 50S  
405 ribosomal protein L5, 50S ribosomal protein L7/L12, 30S ribosomal protein S6; Binds  
406 together with S18 to 16S ribosomal RNA, 50S ribosomal protein L11, 30S ribosomal  
407 protein S7, 50S ribosomal protein L2, Ribosome-recycling factor, and 50S ribosomal  
408 protein L1. Putative virulence-associated proteins, thioredoxin, superoxide dismutase  
409 and molecular chaperones (DnaK, DnaN, GroL, and GrpE) formed another cluster. In  
410 the case of *G. elegans*, DnaK was the only chaperone found. A growing body  
411 of literature [43-45] has shown that a number of enzymes involved in the glycolytic  
412 pathway as well as molecular chaperones are recognized as moonlighting proteins and  
413 thus could play a role in the pathogenesis of bacterial infection. Of the glycolytic  
414 enzymes detected in EVs proteomes in this study, glyceraldehyde-3-phosphate  
415 dehydrogenase, glucose-6-phosphate isomerase, phosphoglycerate kinase, pyruvate  
416 kinase, and ATP-dependent 6-phosphofructokinase were found to possess  
417 moonlighting properties. These enzymes could function as transferrin receptor, cell  
418 signaling kinase, neutrophil evasion protein, immunomodulator, plasminogen binding  
419 protein, fibrinogen binding protein, actin binding protein, and has a role in NAD-  
420 ribosylation activity and extracellular polysaccharide synthesis [44]. Moreover, the  
421 molecular chaperone DnaK was found to act as a multifunctional protein, which could  
422 stimulate CD8 lymphocyte and monocyte chemokines production, compete with HIV  
423 for binding to CCR5 receptors, and bind plasminogen [44]. In addition, it was  
424 concluded by a previous study [47] that many bacterial ribosomal proteins could  
425 function beyond their primary role as ribosomes, integral components of protein  
426 synthesis machinery. These proteins could also modulate different cell processes, such

427 as transcription, regulation of the mRNA stability, DNA repair and replication, and  
428 phage RNA replication [47]. Furthermore, the L7/L12 ribosomal protein was  
429 experimentally proven to elicit a cell-mediated immune response in mice [48].

430

431 **Fig 5. Functional protein association networks of *G. adiacens* EVs proteome.** The  
432 online tool STRING was used for grouping the EVs proteins based on functional  
433 networks. Minimum interaction scores were set at a strong confidence level of 0.7. The  
434 three major network groups formed are shown in dotted circles. Seven different colors  
435 link a number of nodes and represent seven types of evidence used in predicting  
436 associations. A red line indicates the presence of fusion evidence; a green line  
437 represents neighborhood evidence; a blue line represents co-occurrence evidence; a  
438 purple line represents experimental evidence; a yellow line represents text mining  
439 evidence; a light blue line represents database evidence and a black line represents co-  
440 expression evidence.

441

442 **Fig 6. Functional protein association networks of *G. elegans* EVs proteome.** The  
443 online tool STRING was used for grouping the EVs proteins based on functional  
444 networks. Minimum interaction scores were set at a strong confidence level of 0.7. The  
445 three major network groups formed are shown in dotted circles. Seven different colors  
446 link a number of nodes and represent seven types of evidence used in predicting  
447 associations. A red line indicates the presence of fusion evidence; a green line  
448 represents neighborhood evidence; a blue line represents co-occurrence evidence; a  
449 purple line represents experimental evidence; a yellow line represents text mining  
450 evidence; a light blue line represents database evidence and a black line represents co-  
451 expression evidence.

452

453 KEGG pathway analysis of the EVs proteomes is depicted in Fig 7. Proteins  
454 belonging to carbohydrate metabolism and genetic information processing were found  
455 to be the most predominant in *G. adiacens* and *G. elegans* EVs. About 37% of the  
456 proteins in *G. adiacens* EVs proteome was predicted to be involved in the carbohydrate  
457 metabolism and 25% in genetic information processing. On the contrary, *G. elegans*  
458 had the majority (37%) of the EVs proteins in the genetic information processing  
459 category followed by 23% in the carbohydrate metabolism category. As predicted by  
460 the pathway tool, a few proteins from both species were also implicated in amino acid  
461 metabolism, lipid metabolism, glycan metabolism, and energy metabolism. Vesicles  
462 equipped with metabolic machineries can help bacterial colonization and host cell  
463 invasion. For example, ATP generated in vesicles might regulate the activity of  
464 virulence factors and facilitate cell-cell communication of bacteria [49]. Overall,  
465 metabolism related proteins in the EVs might facilitate long-term contact between the  
466 bacterium and the epithelial cells, causing increased epithelial cell/tissue damage.

467

468 **Fig 7. KEGG pathway analysis of the EVs proteomes.** All protein sequences from  
469 *G. adiacens* and *G. elegans* vesicle proteomes were subject to KEGG pathway analysis  
470 using the genus “streptococcus” as reference.

471

## 472 **Prediction of virulence proteins in the EVs proteomes**

473 Our study revealed that EVs produced by both *Granulicatella* species contained  
474 proteins that were predicted to carry virulent properties. This finding overemphasizes  
475 the role of EVs in the pathogenesis of *Granulicatella* infections. Tables 2 and 3 show

476 the list of 44 and 31 proteins that were predicted to be virulent from EVs proteomes of  
477 *G. adiacens* and *G. elegans*, respectively. The major proteins with demonstrated  
478 evidence on their virulence properties in other bacterial species were: thioredoxin [50],  
479 aminopeptidase [51], molecular chaperones DnaK and GroES [52, 53], Superoxide  
480 dismutase [54], Glyceraldehyde-3-phosphate dehydrogenase [55], phosphoglycerate  
481 kinase [56], and acyl carrier protein [57]. A vast literature on membrane vesicles has  
482 demonstrated that a number of well-known and extensively studied toxins and non-  
483 toxin virulence factors are secreted via vesicles [58]. Unlike virulence factors secreted  
484 in soluble form, vesicle-associated virulence factors are provided with a unique benefit  
485 of being protected from host proteases [13]. Moreover, vesicle-virulence factors are  
486 delivered to host cells/tissues as concentrated packages, increasing the damage level at  
487 specific target sites. Vesicle-mediated delivery of virulence factors is a widespread  
488 mechanism across bacterial species and genera. Similar to other oral bacteria such as  
489 *Aggregatibacter actinomycetemcomitans* [59], *Kingella kingae* [60] and others that are  
490 also implicated in infective endocarditis, *Granulicatella* species possibly use their EVs  
491 filled with numerous putative virulent proteins in the pathogenesis of this infection.  
492

493 **Table 2. Putative virulence factors predicted in *G. adiacens* EVs proteome**

GI Number	Protein	Literature evidence
gi 491800464	2-C-methyl-D-erythritol 4-phosphate cytidyltransferase	[61]
gi 748591047	50S ribosomal protein L2	[62]
gi 497579773	ABC transporter permease	[63]
gi 746420217	Abortive infection protein	[64]
gi 491797310	Acyl carrier protein	[57]
gi 491800704	Aminopeptidase	[51]
gi 902780562	AsnC family transcriptional regulator	[65]
gi 491800441	Superoxide dismutase	[54]
gi 491800929	Molecular chaperone DnaK	[52]
gi 496272578	BolA family transcriptional regulator	[66]
gi 748591019	C69 family dipeptidase	[67]
gi 491800219	CHAP domain-containing protein	[68]
gi 763046713	Copper resistance protein CopC	[69]
gi 491799853	DNA starvation/stationary phase protection protein	[70]
gi 930427599	Excalibur calcium-binding domain-containing protein	[71]
gi 491797269	Extracellular solute-binding protein	
gi 696562087	Ferric iron uptake transcriptional regulator	[72]
gi 653213384	GtrA family protein	[73]
gi 944540129	HAMP domain-containing protein	
gi 499448954	Hemagglutinin	
gi 259035990	Phosphoglycerate Kinase	[56]
gi 494465474	Lrp/AsnC family transcriptional regulator	[74]
gi 491801017	LysM peptidoglycan-binding domain-containing protein	[75]
gi 491800929	Molecular chaperone GroES	[53]
gi 873244974	Nucleoside kinase	[76]
gi 544852859	Nucleotidyl transferase	
gi 746564572	PAAR domain-containing protein, partial	[77]
gi 491797885	Phosphonate ABC transporter substrate-binding protein	[78]
gi 922002434	SDR family NAD(P)-dependent oxidoreductase	[79]
gi 500072582	SDR family oxidoreductase	[79]
gi 491797024	Toxic anion resistance protein	
gi 1011464073	Type II secretion system protein GspF	[80]
gi 447107851	Zinc ribbon domain-containing protein, partial	[81]

494

495

496 **Table 3. Putative virulence factors predicted in *G. elegans* EVs proteome.**

GI Number	Protein	Literature evidence
gi 487747677	50S ribosomal protein L2	[62]
gi 488381306	Cell-wall-binding lipoprotein	
gi 488382304	DNA starvation/stationary phase protection protein	[70]
gi 495737870	DoxX family membrane protein	
gi 930427599	Excalibur calcium-binding domain-containing protein	[71]
gi 494255427	HAMP domain-containing protein	[82]
gi 259036192	Thioredoxin	[50]
gi 491800797	Glyceraldehyde-3-phosphate dehydrogenase	[55]
gi 491800929	Molecular chaperone GroES	[53]
gi 491800929	Molecular chaperone DnaK	[52]
gi 935538309	Ig-like domain repeat protein	
gi 736145212	IS630 family transposase	
gi 494465474	Lrp/AsnC family transcriptional regulator	[74]
gi 488363577	LytR family transcriptional regulator	[83]
gi 1011348477	Phosphatidylinositol-specific phospholipase C domain-containing protein	[84]
gi 502784507	SDR family oxidoreductase	[79]
gi 1011513948	Sensor histidine kinase	[85]
gi 640731033	SMI1/KNR4 family protein	
gi 488822607	Type II toxin-antitoxin system HicA family toxin	[86]
gi 446212445	YlbF/YmcA family competence regulator	[87]
gi 505200229	YSIRK-type signal peptide-containing protein, partial	[88]

497

498 **ELISA quantification of selected cytokines produced from**  
 499 **stimulated human PBMCs with EVs and WCP**

500 As shown in Figures 8 and 9, all concentrations (10, 25, 50, and 100 µg/ml) of  
 501 *G. adiacens* EVs, and *G. elegans* EVs triggered the production of the selected potent  
 502 proinflammatory cytokines from human PBMCs as compared to the controls (0 µg/ml).  
 503 Our study demonstrated that both *G. adiacens* EVs and *G. elegans* EVs were able to  
 504 stimulate cytokine release from human PBMCs and thus could play a role in the  
 505 induction of an inflammatory response. This finding is in accordance with previous

506 studies [11, 14, 18, 89] that revealed the immuno-modulatory effects of EVs in other  
507 bacteria. In the current study, EVs from both species induced IL-8 and IL-1 $\beta$ , but not  
508 CCL5, in a dose-dependent manner. *G. adiacens* EVs induced the release of IL-8 and  
509 IL-1 $\beta$  to significantly ( $P < 0.05$ ) higher levels compared to WCP (Fig 8). In the case of  
510 *G. elegans*, compared to WCP, EVs induced significantly higher levels of only the IL-  
511 1 $\beta$  ( $P < 0.05$ ) (Fig 9). When cytokine levels were compared between the two species,  
512 no statistically significant difference was found. These observations overemphasize the  
513 importance of bacterial vesicle production in the activation of inflammation and thus  
514 pathogenesis of bacterial infections. The ability of bacterial vesicles to trigger host  
515 inflammatory response is a well-established phenomenon. When host epithelial cells  
516 encounter or take up the vesicles, an immediate innate immune response begins. IL-8  
517 and IL-1 $\beta$  are prominent cytokines in infective endocarditis [90], but also in oral  
518 infections [91, 92]. IL-1 $\beta$  has a wide range of actions mediating inflammatory host  
519 response. At low concentrations, it mediates local inflammation while at high  
520 concentrations it possesses endocrine effects. Due to its neutrophil recruiting property,  
521 IL-8 is a major inflammatory cytokine induced by a variety of microbial components  
522 [93, 94].

523

524 **Fig 8. ELISA quantification of IL-8 (A), IL-1 $\beta$  (B), and CCL5 (C) production by**  
525 **human PBMCs stimulated with *G. adiacens* EVs and WCP (10, 25, 50, and 100**  
526  **$\mu$ g/ml). EVs induction was considered significantly different from WCP induction at**  
527 **\* $p < 0.05$ .**

528

529 **Fig 9. ELISA quantification of IL-8 (A), IL-1 $\beta$  (B), and CCL5 (C) production by**  
530 **human PBMCs stimulated with *G. elegans* EVs and WCP (10, 25, 50, and 100**



531  $\mu\text{g/ml}$ ). EVs induction was considered significantly different from WCP induction at  
532  $*p < 0.05$ .

## 533 **Conclusion**

534 To the best of our knowledge, this is the first research that presented evidence  
535 for the hypothesis that *Granulicatella* species release EVs. We discovered that the EVs  
536 proteomes of *G. adiacens* and *G. elegans* were enriched with a large number of  
537 predicted putative virulence factors. *Granulicatella* species possibly use their EVs as  
538 vehicles to deliver virulence factors to body sites not accessible to whole bacterial  
539 cells—a mechanism widespread across bacterial species. In addition to virulent  
540 proteins, which can impose direct detrimental effects on host cells/tissues, other  
541 components of the EVs, i.e., metabolic enzymes, ribosomal proteins, stress-response  
542 proteins may contribute to pathogenesis by enhancing adaptation of these species and  
543 survival in the hostile host environments. Thus, the diversity in EVs content emphasizes  
544 the possible roles of these vesicles in bacterial survival, invasion, host immune  
545 modulation as well as infection. Moreover, EVs of both species were demonstrated to  
546 be potent inducers of proinflammatory cytokines, and importantly, the EVs were  
547 significantly more potent than the whole cell proteins in eliciting inflammatory  
548 response. These EVs may play an important role in the activation of inflammation and  
549 thus pathogenesis of *Granulicatella* infections. Further functional characterization of  
550 the *Granulicatella* EVs may throw more light on how these species may utilize vesicles  
551 to orchestrate events that may lead them from being silent normal flora species towards  
552 infection-causing ones.

553

## 554 **Acknowledgments**

555           This study was supported by Kuwait University Grant SRUL 01/14 and partly  
556 by the College of Graduate Studies, Kuwait University. Special gratitude is given to the  
557 Research Core Facility, Health Sciences Center, Kuwait University, the Department of  
558 Microbiology, Faculty of Medicine, Kuwait University, and The Nanoscopy Science  
559 Center, Faculty of Science, Kuwait University for the permission to use their facilities.  
560

561

## 562 References

- 563 1. Ruoff KL. Nutritionally variant streptococci. Clin Microbiol Rev.  
564 1991;4(2):184-90. Epub 1991/04/01. PMID: 2070344.
- 565 2. Cargill JS, Scott KS, Gascoyne-Binzi D, Sandoe JA. *Granulicatella* infection:  
566 diagnosis and management. J Med Microbiol. 2012;61(Pt 6):755-61. Epub  
567 2012/03/24. doi: 10.1099/jmm.0.039693-0. PMID: 22442291.
- 568 3. Collins MD, Lawson PA. The genus *Abiotrophia* (Kawamura et al.) is not  
569 monophyletic: proposal of *Granulicatella* gen. nov., *Granulicatella adiacens*  
570 comb. nov., *Granulicatella elegans* comb. nov. and *Granulicatella*  
571 *balaenopterae* comb. nov. Int J Syst Evol Microbiol. 2000;50 Pt 1:365-9. Epub  
572 2000/05/29. doi: 10.1099/00207713-50-1-365. PMID: 10826824.
- 573 4. Aas JA, Paster BJ, Stokes LN, Olsen I, Dewhirst FE. Defining the normal  
574 bacterial flora of the oral cavity. J Clin Microbiol. 2005;43(11):5721-32. Epub  
575 2005/11/08. doi: 10.1128/jcm.43.11.5721-5732.2005. PMID: 16272510.
- 576 5. Adam EL, Siciliano RF, Gualandro DM, Calderaro D, Issa VS, Rossi F, et al.  
577 Case series of infective endocarditis caused by *Granulicatella* species. Int J  
578 Infect Dis. 2015;31:56-8. Epub 2014/12/03. doi: 10.1016/j.ijid.2014.10.023.  
579 PMID: 25461651.
- 580 6. Giuliano S, Caccese R, Carfagna P, Vena A, Falcone M, Venditti M.  
581 Endocarditis caused by nutritionally variant streptococci: a case report and  
582 literature review. Infez Med. 2012;20(2):67-74. Epub 2012/07/07. PMID:  
583 22767303.
- 584 7. Hsiao WW, Li KL, Liu Z, Jones C, Fraser-Liggett CM, Fouad AF. Microbial  
585 transformation from normal oral microbiota to acute endodontic infections.  
586 BMC Genomics. 2012;13:345. Epub 2012/07/31. doi: 10.1186/1471-2164-13-  
587 345. PMID: 22839737.
- 588 8. Siqueira JF, Jr., Rocas IN. *Catonella morbi* and *Granulicatella adiacens*: new  
589 species in endodontic infections. Oral Surg Oral Med Oral Pathol Oral Radiol  
590 Endod. 2006;102(2):259-64. Epub 2006/08/01. doi:  
591 10.1016/j.tripleo.2005.09.021. PMID: 16876072.
- 592 9. Kanasi E, Dewhirst FE, Chalmers NI, Kent R, Jr., Moore A, Hughes CV, et al.  
593 Clonal analysis of the microbiota of severe early childhood caries. Caries Res.  
594 2010;44(5):485-97. Epub 2010/09/24. doi: 10.1159/000320158. PMID:  
595 20861633.
- 596 10. Asikainen S, Dogan B, Turgut Z, Paster BJ, Bodur A, Oscarsson J. Specified  
597 species in gingival crevicular fluid predict bacterial diversity. PLoS One.  
598 2010;5(10):e13589. Epub 2010/11/05. doi: 10.1371/journal.pone.0013589.  
599 PMID: 21049043.
- 600 11. Schwab A, Meyering SS, Lepene B, Iordanskiy S, van Hoek ML, Hakami RM,  
601 et al. Extracellular vesicles from infected cells: potential for direct pathogenesis.  
602 Front Microbiol. 2015;6:1132. Epub 2015/11/06. doi:  
603 10.3389/fmicb.2015.01132. PMID: 26539170.
- 604 12. Ellis TN, Kuehn MJ. Virulence and immunomodulatory roles of bacterial outer  
605 membrane vesicles. Microbiol Mol Biol Rev. 2010;74(1):81-94. Epub  
606 2010/03/04. doi: 10.1128/mmbr.00031-09. PMID: 20197500.

- 607 13. Kuehn MJ, Kesty NC. Bacterial outer membrane vesicles and the host-pathogen  
608 interaction. *Genes Dev.* 2005;19(22):2645-55. Epub 2005/11/18. doi:  
609 10.1101/gad.1299905. PMID: 16291643.
- 610 14. Avila-Calderon ED, Araiza-Villanueva MG, Cancino-Diaz JC, Lopez-Villegas  
611 EO, Sriranganathan N, Boyle SM, et al. Roles of bacterial membrane vesicles.  
612 *Arch Microbiol.* 2015;197(1):1-10. Epub 2014/10/09. doi: 10.1007/s00203-  
613 014-1042-7. PMID: 25294190.
- 614 15. Brown L, Wolf JM, Prados-Rosales R, Casadevall A. Through the wall:  
615 extracellular vesicles in Gram-positive bacteria, mycobacteria and fungi. *Nat*  
616 *Rev Microbiol.* 2015;13(10):620-30. Epub 2015/09/02. doi:  
617 10.1038/nrmicro3480. PMID: 26324094.
- 618 16. Kim GH, Choi CW, Park EC, Lee SY, Kim SI. Isolation and proteomic  
619 characterization of bacterial extracellular membrane vesicles. *Curr Protein Pept*  
620 *Sci.* 2014;15(7):719-31. Epub 2014/05/08. PMID: 24800937.
- 621 17. Kim JH, Lee J, Park J, Gho YS. Gram-negative and Gram-positive bacterial  
622 extracellular vesicles. *Semin Cell Dev Biol.* 2015;40:97-104. Epub 2015/02/24.  
623 doi: 10.1016/j.semcdb.2015.02.006. PMID: 25704309.
- 624 18. Liu Y, Defourny KAY, Smid EJ, Abee T. Gram-Positive Bacterial Extracellular  
625 Vesicles and Their Impact on Health and Disease. *Front Microbiol.*  
626 2018;9:1502. Epub 2018/07/25. doi: 10.3389/fmicb.2018.01502. PMID:  
627 30038605.
- 628 19. Toyofuku M, Carcamo-Oyarce G, Yamamoto T, Eisenstein F, Hsiao CC,  
629 Kurosawa M, et al. Prophage-triggered membrane vesicle formation through  
630 peptidoglycan damage in *Bacillus subtilis*. *Nat Commun.* 2017;8(1):481. Epub  
631 2017/09/09. doi: 10.1038/s41467-017-00492-w. PMID: 28883390.
- 632 20. Wang X, Thompson CD, Weidenmaier C, Lee JC. Release of *Staphylococcus*  
633 *aureus* extracellular vesicles and their application as a vaccine platform. *Nat*  
634 *Commun.* 2018;9(1):1379. Epub 2018/04/13. doi: 10.1038/s41467-018-03847-  
635 z. PMID: 29643357.
- 636 21. Karched M, Bhardwaj RG, Tiss A, Asikainen S. Proteomic Analysis and  
637 Virulence Assessment of *Granulicatella adiacens* Secretome. 2019;9(104). doi:  
638 10.3389/fcimb.2019.00104.
- 639 22. Karched M, Ihalin R, Eneslatt K, Zhong D, Oscarsson J, Wai SN, et al. Vesicle-  
640 independent extracellular release of a proinflammatory outer membrane  
641 lipoprotein in free-soluble form. *BMC Microbiol.* 2008;8:18. Epub 2008/01/30.  
642 doi: 10.1186/1471-2180-8-18. PMID: 18226201.
- 643 23. Hiller K, Schobert M, Hundertmark C, Jahn D, Munch R. JVirGel: Calculation  
644 of virtual two-dimensional protein gels. *Nucleic Acids Res.* 2003;31(13):3862-  
645 5. Epub 2003/06/26. PMID: 12824438.
- 646 24. Yu NY, Wagner JR, Laird MR, Melli G, Rey S, Lo R, et al. PSORTb 3.0:  
647 improved protein subcellular localization prediction with refined localization  
648 subcategories and predictive capabilities for all prokaryotes. *Bioinformatics.*  
649 2010;26(13):1608-15. Epub 2010/05/18. doi: 10.1093/bioinformatics/btq249.  
650 PMID: 20472543.
- 651 25. Almagro Armenteros JJ, Tsirigos KD, Sonderby CK, Petersen TN, Winther O,  
652 Brunak S, et al. SignalP 5.0 improves signal peptide predictions using deep  
653 neural networks. *Nat Biotechnol.* 2019;37(4):420-3. Epub 2019/02/20. doi:  
654 10.1038/s41587-019-0036-z. PMID: 30778233.

- 655 26. Bendtsen JD, Nielsen H, Widdick D, Palmer T, Brunak S. Prediction of twin-  
656 arginine signal peptides. *BMC Bioinformatics*. 2005;6:167. Epub 2005/07/05.  
657 doi: 10.1186/1471-2105-6-167. PMID: 15992409.
- 658 27. Bagos PG, Tsirigos KD, Liakopoulos TD, Hamodrakas SJ. Prediction of  
659 lipoprotein signal peptides in Gram-positive bacteria with a Hidden Markov  
660 Model. *J Proteome Res*. 2008;7(12):5082-93. Epub 2009/04/16. doi:  
661 10.1021/pr800162c. PMID: 19367716.
- 662 28. Chen C, Zabad S, Liu H, Wang W, Jeffery C. MoonProt 2.0: an expansion and  
663 update of the moonlighting proteins database. *Nucleic Acids Res*.  
664 2018;46(D1):D640-d4. Epub 2017/11/11. doi: 10.1093/nar/gkx1043. PMID:  
665 29126295.
- 666 29. Franco-Serrano L, Hernandez S, Calvo A, Severi MA, Ferragut G, Perez-Pons  
667 J, et al. MultitaskProtDB-II: an update of a database of  
668 multitasking/moonlighting proteins. *Nucleic Acids Res*. 2018;46(D1):D645-d8.  
669 Epub 2017/11/15. doi: 10.1093/nar/gkx1066. PMID: 29136215.
- 670 30. Conesa A, Gotz S, Garcia-Gomez JM, Terol J, Talon M, Robles M. Blast2GO:  
671 a universal tool for annotation, visualization and analysis in functional genomics  
672 research. *Bioinformatics*. 2005;21(18):3674-6. Epub 2005/08/06. doi:  
673 10.1093/bioinformatics/bti610. PMID: 16081474.
- 674 31. Ye J, Zhang Y, Cui H, Liu J, Wu Y, Cheng Y, et al. WEGO 2.0: a web tool for  
675 analyzing and plotting GO annotations, 2018 update. *Nucleic Acids Res*.  
676 2018;46(W1):W71-w5. Epub 2018/05/23. doi: 10.1093/nar/gky400. PMID:  
677 29788377.
- 678 32. von Mering C, Jensen LJ, Snel B, Hooper SD, Krupp M, Foglierini M, et al.  
679 STRING: known and predicted protein-protein associations, integrated and  
680 transferred across organisms. *Nucleic Acids Res*. 2005;33(Database  
681 issue):D433-7. Epub 2004/12/21. doi: 10.1093/nar/gki005. PMID: 15608232.  
682
- 683 33. Du J, Yuan Z, Ma Z, Song J, Xie X, Chen Y. KEGG-PATH: Kyoto  
684 encyclopedia of genes and genomes-based pathway analysis using a path  
685 analysis model. *Mol Biosyst*. 2014;10(9):2441-7. Epub 2014/07/06. doi:  
686 10.1039/c4mb00287c. PMID: 24994036.
- 687 34. Garg A, Gupta D. VirulentPred: a SVM based prediction method for virulent  
688 proteins in bacterial pathogens. *BMC Bioinformatics*. 2008;9:62. Epub  
689 2008/01/30. doi: 10.1186/1471-2105-9-62. PMID: 18226234.
- 690 35. Bhardwaj RG, Al-Khabbaz A, Karched M. Cytokine induction of peripheral  
691 blood mononuclear cells by biofilms and biofilm supernatants of *Granulicatella*  
692 and *Abiotrophia* spp. *Microb Pathog*. 2018;114:90-4. Epub 2017/11/28. doi:  
693 10.1016/j.micpath.2017.11.037. PMID: 29174702.
- 694 36. Haas B, Grenier D. Isolation, Characterization and Biological Properties of  
695 Membrane Vesicles Produced by the Swine Pathogen *Streptococcus suis*. *PLoS*  
696 *One*. 2015;10(6):e0130528. Epub 2015/06/26. doi:  
697 10.1371/journal.pone.0130528. PMID: 26110524.
- 698 37. Kim Y, Edwards N, Fenselau C. Extracellular vesicle proteomes reflect  
699 developmental phases of *Bacillus subtilis*. *Clin Proteomics*. 2016;13:6. Epub  
700 2016/03/11. doi: 10.1186/s12014-016-9107-z. PMID: 26962304.
- 701 38. Resch U, Tsatsaronis JA, Le Rhun A, Stübiger G, Rohde M, Kasvandik S, et al.  
702 A Two-Component Regulatory System Impacts Extracellular Membrane-  
703 Derived Vesicle Production in Group A *Streptococcus*. *MBio*. 2016;7(6). Epub  
704 2016/11/03. doi: 10.1128/mBio.00207-16. PMID: 27803183.

- 705 39. Bai J, Kim SI, Ryu S, Yoon H. Identification and characterization of outer  
706 membrane vesicle-associated proteins in *Salmonella enterica* serovar  
707 *Typhimurium*. *Infect Immun*. 2014;82(10):4001-10. Epub 2014/06/18. doi:  
708 10.1128/iai.01416-13. PMID: 24935973.
- 709 40. Ebner P, Gotz F. Bacterial Excretion of Cytoplasmic Proteins (ECP):  
710 Occurrence, Mechanism, and Function. *Trends Microbiol*. 2019;27(2):176-87.  
711 Epub 2018/11/18. doi: 10.1016/j.tim.2018.10.006. PMID: 30442534.
- 712 41. Green ER, Meccas J. Bacterial Secretion Systems: An Overview. *Microbiol*  
713 *Spectr*. 2016;4(1). Epub 2016/03/22. doi: 10.1128/microbiolspec.VMBF-0012-  
714 2015. PMID: 26999395.
- 715 42. Natale P, Bruser T, Driessen AJ. Sec- and Tat-mediated protein secretion across  
716 the bacterial cytoplasmic membrane--distinct translocases and mechanisms.  
717 *Biochim Biophys Acta*. 2008;1778(9):1735-56. Epub 2007/10/16. doi:  
718 10.1016/j.bbamem.2007.07.015. PMID: 17935691.
- 719 43. Henderson B. An overview of protein moonlighting in bacterial infection.  
720 *Biochem Soc Trans*. 2014;42(6):1720-7. doi: 10.1042/BST20140236. PMID:  
721 25399596.
- 722 44. Henderson B, Martin A. Bacterial virulence in the moonlight: multitasking  
723 bacterial moonlighting proteins are virulence determinants in infectious disease.  
724 *Infect Immun*. 2011;79(9):3476-91. Epub 2011/06/08. doi: 10.1128/iai.00179-  
725 11. PMID: 21646455.
- 726 45. Henderson B, Martin A. Bacterial moonlighting proteins and bacterial  
727 virulence. *Curr Top Microbiol Immunol*. 2013;358:155-213. Epub 2011/12/07.  
728 doi: 10.1007/82\_2011\_188. PMID: 22143554.
- 729 46. Cezairliyan B, Ausubel FM. Investment in secreted enzymes during nutrient-  
730 limited growth is utility dependent. *Proc Natl Acad Sci U S A*.  
731 2017;114(37):E7796-e802. Epub 2017/08/30. doi: 10.1073/pnas.1708580114.  
732 PMID: 28847943.
- 733 47. Aseev LV, Boni IVJMB. Extraribosomal functions of bacterial ribosomal  
734 proteins. 2011;45(5):739. doi: 10.1134/s0026893311050025.
- 735 48. Oliveira SC, Harms JS, Banai M, Splitter GA. Recombinant *Brucella abortus*  
736 proteins that induce proliferation and gamma-interferon secretion by CD4+ T  
737 cells from *Brucella*-vaccinated mice and delayed-type hypersensitivity in  
738 sensitized guinea pigs. *Cell Immunol*. 1996;172(2):262-8. Epub 1996/09/15.  
739 doi: 10.1006/cimm.1996.0241. PMID: 8964089.
- 740 49. Zakharzhevskaya NB, Vanyushkina AA, Altukhov IA, Shavarda AL, Butenko  
741 IO, Rakitina DV, et al. Outer membrane vesicles secreted by pathogenic and  
742 nonpathogenic *Bacteroides fragilis* represent different metabolic activities. *Sci*  
743 *Rep*. 2017;7(1):5008. Epub 2017/07/12. doi: 10.1038/s41598-017-05264-6.  
744 PMID: 28694488.
- 745 50. Bjur E, Eriksson-Ygberg S, Aslund F, Rhen M. Thioredoxin 1 promotes  
746 intracellular replication and virulence of *Salmonella enterica* serovar  
747 *Typhimurium*. *Infect Immun*. 2006;74(9):5140-51. Epub 2006/08/24. doi:  
748 10.1128/iai.00449-06. PMID: 16926406.
- 749 51. Carroll RK, Robison TM, Rivera FE, Davenport JE, Jonsson IM, Florczyk D,  
750 et al. Identification of an intracellular M17 family leucine aminopeptidase that  
751 is required for virulence in *Staphylococcus aureus*. *Microbes Infect*.  
752 2012;14(11):989-99. Epub 2012/05/23. doi: 10.1016/j.micinf.2012.04.013.  
753 PMID: 22613209.



- 754 52. Goulhen F, Hafezi A, Uitto VJ, Hinode D, Nakamura R, Grenier D, et al.  
755 Subcellular localization and cytotoxic activity of the GroEL-like protein  
756 isolated from *Actinobacillus actinomycetemcomitans*. Infect Immun.  
757 1998;66(11):5307-13. Epub 1998/10/24. PMID: 9784537.
- 758 53. Hinode D, Grenier D, Mayrand D. Purification and characterization of a DnaK-  
759 like and a GroEL-like protein from *Porphyromonas gingivalis*. Anaerobe.  
760 1995;1(5):283-90. Epub 1995/10/01. doi: 10.1006/anae.1995.1028. PMID:  
761 16887537.
- 762 54. Gerlach D, Reichardt W, Vettermann S. Extracellular superoxide dismutase  
763 from *Streptococcus pyogenes* type 12 strain is manganese-dependent. FEMS  
764 Microbiol Lett. 1998;160(2):217-24. Epub 1998/04/09. doi: 10.1111/j.1574-  
765 6968.1998.tb12914.x. PMID: 9532741.
- 766 55. Lu GT, Xie JR, Chen L, Hu JR, An SQ, Su HZ, et al. Glyceraldehyde-3-  
767 phosphate dehydrogenase of *Xanthomonas campestris* pv. *campestris* is  
768 required for extracellular polysaccharide production and full virulence.  
769 Microbiology. 2009;155(Pt 5):1602-12. Epub 2009/04/18. doi:  
770 10.1099/mic.0.023762-0. PMID: 19372163.
- 771 56. Baska P, Norbury LJ, Wisniewski M, Januszkiewicz K, Wedrychowicz H.  
772 Excretory/secretory products of *Fasciola hepatica* but not recombinant  
773 phosphoglycerate kinase induce death of human hepatocyte cells. Acta  
774 Parasitol. 2013;58(2):215-7. Epub 2013/05/15. doi: 10.2478/s11686-013-0126-  
775 x. PMID: 23666658.
- 776 57. Taguchi F, Ogawa Y, Takeuchi K, Suzuki T, Toyoda K, Shiraishi T, et al. A  
777 homologue of the 3-oxoacyl-(acyl carrier protein) synthase III gene located in  
778 the glycosylation island of *Pseudomonas syringae* pv. *tabaci* regulates virulence  
779 factors via N-acyl homoserine lactone and fatty acid synthesis. J Bacteriol.  
780 2006;188(24):8376-84. Epub 2006/10/10. doi: 10.1128/jb.00763-06. PMID:  
781 17028280.
- 782 58. Schwechheimer C, Kuehn MJ. Outer-membrane vesicles from Gram-negative  
783 bacteria: biogenesis and functions. Nat Rev Microbiol. 2015;13(10):605-19.  
784 Epub 2015/09/17. doi: 10.1038/nrmicro3525. PMID: 26373371.
- 785 59. Thay B, Damm A, Kufer TA, Wai SN, Oscarsson J. *Aggregatibacter*  
786 *actinomycetemcomitans* outer membrane vesicles are internalized in human  
787 host cells and trigger NOD1- and NOD2-dependent NF-kappaB activation.  
788 Infect Immun. 2014;82(10):4034-46. Epub 2014/07/16. doi: 10.1128/iai.01980-  
789 14. PMID: 25024364.
- 790 60. Maldonado R, Wei R, Kachlany SC, Kazi M, Balashova NV. Cytotoxic effects  
791 of *Kingella kingae* outer membrane vesicles on human cells. Microb Pathog.  
792 2011;51(1-2):22-30. Epub 2011/03/30. doi: 10.1016/j.micpath.2011.03.005.  
793 PMID: 21443941.
- 794 61. Tsang A, Seidle H, Jawaid S, Zhou W, Smith C, Couch RD. *Francisella*  
795 *tularensis* 2-C-methyl-D-erythritol 4-phosphate cytidyltransferase: kinetic  
796 characterization and phosphoregulation. PLoS One. 2011;6(6):e20884. Epub  
797 2011/06/23. doi: 10.1371/journal.pone.0020884. PMID: 21694781.
- 798 62. Singh I, Yadav AR, Mohanty KK, Katoch K, Sharma P, Mishra B, et al.  
799 Molecular mimicry between *Mycobacterium leprae* proteins (50S ribosomal  
800 protein L2 and Lysyl-tRNA synthetase) and myelin basic protein: a possible  
801 mechanism of nerve damage in leprosy. Microbes Infect. 2015;17(4):247-57.  
802 Epub 2015/01/13. doi: 10.1016/j.micinf.2014.12.015. PMID: 25576930.

- 803 63. Garmory HS, Titball RW. ATP-binding cassette transporters are targets for the  
804 development of antibacterial vaccines and therapies. *Infect Immun.*  
805 2004;72(12):6757-63. Epub 2004/11/24. doi: 10.1128/iai.72.12.6757-  
806 6763.2004. PMID: 15557595.
- 807 64. Haaber J, Samson JE, Labrie SJ, Campanacci V, Cambillau C, Moineau S, et al.  
808 Lactococcal abortive infection protein AbiV interacts directly with the phage  
809 protein SaV and prevents translation of phage proteins. *Appl Environ*  
810 *Microbiol.* 2010;76(21):7085-92. Epub 2010/09/21. doi: 10.1128/aem.00093-  
811 10. PMID: 20851990.
- 812 65. Deng W, Wang H, Xie J. Regulatory and pathogenesis roles of *Mycobacterium*  
813 *Lrp/AsnC* family transcriptional factors. *J Cell Biochem.* 2011;112(10):2655-  
814 62. Epub 2011/05/25. doi: 10.1002/jcb.23193. PMID: 21608015.
- 815 66. Moreira RN, Dressaire C, Barahona S, Galego L, Kaeffer V, Jenal U, et al. BolA  
816 Is Required for the Accurate Regulation of c-di-GMP, a Central Player in  
817 Biofilm Formation. *MBio.* 2017;8(5). Epub 2017/09/21. doi:  
818 10.1128/mBio.00443-17. PMID: 28928205.
- 819 67. Sakamoto T, Otokawa T, Kono R, Shigeri Y, Watanabe K. A C69-family  
820 cysteine dipeptidase from *Lactobacillus farciminis* JCM1097 possesses strong  
821 Gly-Pro hydrolytic activity. *J Biochem.* 2013;154(5):419-27. Epub 2013/08/30.  
822 doi: 10.1093/jb/mvt069. PMID: 23986487.
- 823 68. Zhong Q, Zhao Y, Chen T, Yin S, Yao X, Wang J, et al. A functional  
824 peptidoglycan hydrolase characterized from T4SS in 89K pathogenicity island  
825 of epidemic *Streptococcus suis* serotype 2. *BMC Microbiol.* 2014;14:73. Epub  
826 2014/03/25. doi: 10.1186/1471-2180-14-73. PMID: 24655418.
- 827 69. Ladomersky E, Petris MJ. Copper tolerance and virulence in bacteria.  
828 *Metallomics.* 2015;7(6):957-64. Epub 2015/02/06. doi: 10.1039/c4mt00327f.  
829 PMID: 25652326.
- 830 70. Loprasert S, Whangsuk W, Sallabhan R, Mongkolsuk S. DpsA protects the  
831 human pathogen *Burkholderia pseudomallei* against organic hydroperoxide.  
832 *Arch Microbiol.* 2004;182(1):96-101. Epub 2004/07/09. doi: 10.1007/s00203-  
833 004-0694-0. PMID: 15241582.
- 834 71. Rigden DJ, Jedrzejewski MJ, Galperin MY. An extracellular calcium-binding  
835 domain in bacteria with a distant relationship to EF-hands. *FEMS Microbiol*  
836 *Lett.* 2003;221(1):103-10. Epub 2003/04/16. doi: 10.1016/s0378-  
837 1097(03)00160-5. PMID: 12694917.
- 838 72. Troxell B, Hassan HM. Transcriptional regulation by Ferric Uptake Regulator  
839 (Fur) in pathogenic bacteria. *Front Cell Infect Microbiol.* 2013;3:59. Epub  
840 2013/10/10. doi: 10.3389/fcimb.2013.00059. PMID: 24106689.
- 841 73. Kolly GS, Mukherjee R, Kilacsikova E, Abriata LA, Raccaud M, Blasko J, et al.  
842 GtrA Protein Rv3789 Is Required for Arabinosylation of Arabinogalactan in  
843 *Mycobacterium tuberculosis*. *J Bacteriol.* 2015;197(23):3686-97. Epub  
844 2015/09/16. doi: 10.1128/jb.00628-15. PMID: 26369580.
- 845 74. Knoten CA, Hudson LL, Coleman JP, Farrow JM, 3rd, Pesci EC. KynR, a  
846 Lrp/AsnC-type transcriptional regulator, directly controls the kynurenine  
847 pathway in *Pseudomonas aeruginosa*. *J Bacteriol.* 2011;193(23):6567-75. Epub  
848 2011/10/04. doi: 10.1128/jb.05803-11. PMID: 21965577.
- 849 75. Shi XZ, Feng XW, Sun JJ, Yang MC, Lan JF, Zhao XF, et al. Involvement of a  
850 LysM and putative peptidoglycan-binding domain-containing protein in the  
851 antibacterial immune response of kuruma shrimp *Marsupenaeus japonicus*. *Fish*

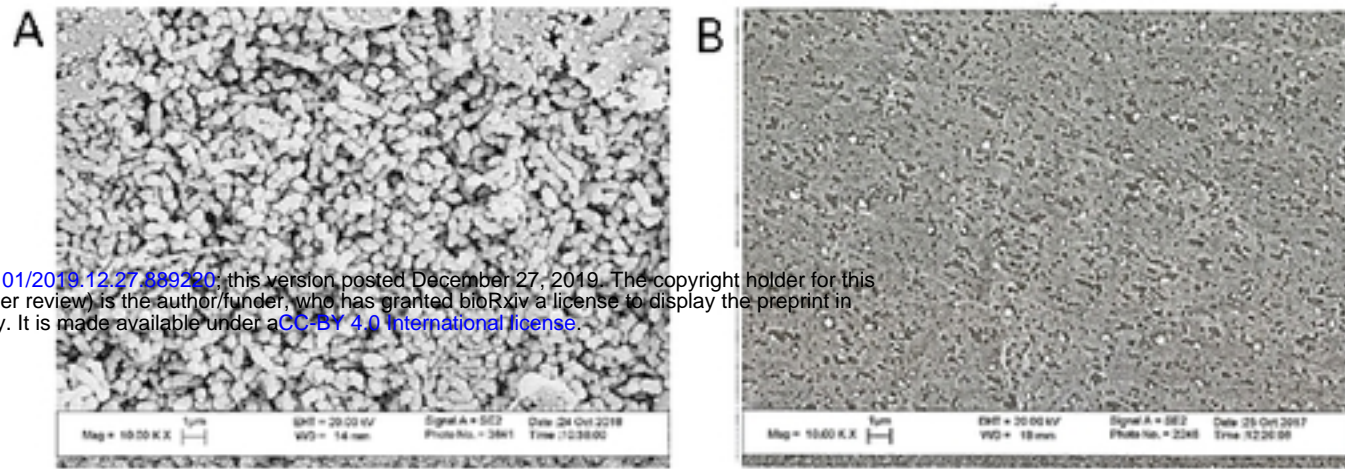


- 852 Shellfish Immunol. 2016;54:489-98. Epub 2016/05/05. doi:  
853 10.1016/j.fsi.2016.04.134. PMID: 27142936.
- 854 76. Chakrabarty AM. Nucleoside diphosphate kinase: role in bacterial growth,  
855 virulence, cell signalling and polysaccharide synthesis. Mol Microbiol.  
856 1998;28(5):875-82. Epub 1998/07/15. PMID: 9663675.
- 857 77. Cianfanelli FR, Alcoforado Diniz J, Guo M, De Cesare V, Trost M, Coulthurst  
858 SJ. VgrG and PAAR Proteins Define Distinct Versions of a Functional Type VI  
859 Secretion System. PLoS Pathog. 2016;12(6):e1005735. Epub 2016/06/29. doi:  
860 10.1371/journal.ppat.1005735. PMID: 27352036.
- 861 78. Tian M, Bao Y, Li P, Hu H, Ding C, Wang S, et al. The putative amino acid  
862 ABC transporter substrate-binding protein AapJ2 is necessary for *Brucella*  
863 virulence at the early stage of infection in a mouse model. Vet Res.  
864 2018;49(1):32. Epub 2018/03/31. doi: 10.1186/s13567-018-0527-9. PMID:  
865 29598830.
- 866 79. Bijtenhoorn P, Mayerhofer H, Muller-Dieckmann J, Utpatel C, Schipper C,  
867 Hornung C, et al. A novel metagenomic short-chain dehydrogenase/reductase  
868 attenuates *Pseudomonas aeruginosa* biofilm formation and virulence on  
869 *Caenorhabditis elegans*. PLoS One. 2011;6(10):e26278. Epub 2011/11/03. doi:  
870 10.1371/journal.pone.0026278. PMID: 22046268.
- 871 80. Cianciotto NP, White RC. Expanding Role of Type II Secretion in Bacterial  
872 Pathogenesis and Beyond. Infect Immun. 2017;85(5). Epub 2017/03/08. doi:  
873 10.1128/iai.00014-17. PMID: 28264910.
- 874 81. Wen J, Liu Y, Liu J, Liu L, Song C, Han J, et al. Expression quantitative trait  
875 loci in long non-coding RNA ZNRD1-AS1 influence both HBV infection and  
876 hepatocellular carcinoma development. Mol Carcinog. 2015;54(11):1275-82.  
877 Epub 2014/08/12. doi: 10.1002/mc.22200. PMID: 25110835.
- 878 82. Khursigara CM, Wu X, Zhang P, Lefman J, Subramaniam S. Role of HAMP  
879 domains in chemotaxis signaling by bacterial chemoreceptors. Proc Natl Acad  
880 Sci U S A. 2008;105(43):16555-60. Epub 2008/10/23. doi:  
881 10.1073/pnas.0806401105. PMID: 18940922.
- 882 83. Galperin MY. Telling bacteria: do not LytTR. Structure. 2008;16(5):657-9.  
883 Epub 2008/05/09. doi: 10.1016/j.str.2008.04.003. PMID: 18462668.
- 884 84. Zenewicz LA, Wei Z, Goldfine H, Shen H. Phosphatidylinositol-specific  
885 phospholipase C of *Bacillus anthracis* down-modulates the immune response. J  
886 Immunol. 2005;174(12):8011-6. Epub 2005/06/10. PMID: 15944308.
- 887 85. Brinkman FS, Macfarlane EL, Warrenner P, Hancock RE. Evolutionary  
888 relationships among virulence-associated histidine kinases. Infect Immun.  
889 2001;69(8):5207-11. Epub 2001/07/12. doi: 10.1128/iai.69.8.5207-5211.2001.  
890 PMID: 11447209.
- 891 86. Lobato-Marquez D, Diaz-Orejas R, Garcia-Del Portillo F. Toxin-antitoxins and  
892 bacterial virulence. FEMS Microbiol Rev. 2016;40(5):592-609. Epub  
893 2016/08/01. doi: 10.1093/femsre/fuw022. PMID: 27476076.
- 894 87. Tortosa P, Albano M, Dubnau D. Characterization of ylbF, a new gene involved  
895 in competence development and sporulation in *Bacillus subtilis*. Mol Microbiol.  
896 2000;35(5):1110-9. Epub 2000/03/11. PMID: 10712692.
- 897 88. Bae T, Schneewind O. The YSIRK-G/S motif of staphylococcal protein A and  
898 its role in efficiency of signal peptide processing. J Bacteriol.  
899 2003;185(9):2910-9. Epub 2003/04/18. doi: 10.1128/jb.185.9.2910-2919.2003.  
900 PMID: 12700270.

- 901 89. MacDonald IA, Kuehn MJ. Offense and defense: microbial membrane vesicles  
902 play both ways. *Res Microbiol.* 2012;163(9-10):607-18. Epub 2012/11/06. doi:  
903 10.1016/j.resmic.2012.10.020. PMID: 23123555.
- 904 90. Araujo IR, Ferrari TC, Teixeira-Carvalho A, Campi-Azevedo AC, Rodrigues  
905 LV, Guimaraes Junior MH, et al. Cytokine Signature in Infective Endocarditis.  
906 *PLoS One.* 2015;10(7):e0133631. Epub 2015/08/01. doi:  
907 10.1371/journal.pone.0133631. PMID: 26225421.
- 908 91. Yamaji Y, Kubota T, Sasaguri K, Sato S, Suzuki Y, Kumada H, et al.  
909 Inflammatory cytokine gene expression in human periodontal ligament  
910 fibroblasts stimulated with bacterial lipopolysaccharides. *Infect Immun.*  
911 1995;63(9):3576-81. Epub 1995/09/01. PMID: 7642293.
- 912 92. Yamamoto T, Kita M, Oseko F, Nakamura T, Imanishi J, Kanamura N.  
913 Cytokine production in human periodontal ligament cells stimulated with  
914 *Porphyromonas gingivalis*. *J Periodontal Res.* 2006;41(6):554-9. Epub  
915 2006/11/02. doi: 10.1111/j.1600-0765.2006.00905.x. PMID: 17076781.
- 916 93. Jiang Y, Russell TR, Schilder H, Graves DT. Endodontic pathogens stimulate  
917 monocyte chemoattractant protein-1 and interleukin-8 in mononuclear cells. *J*  
918 *Endod.* 1998;24(2):86-90. Epub 1998/06/26. doi: 10.1016/s0099-  
919 2399(98)80083-6. PMID: 9641137.
- 920 94. Nagaoka S, Tokuda M, Sakuta T, Taketoshi Y, Tamura M, Takada H, et al.  
921 Interleukin-8 gene expression by human dental pulp fibroblast in cultures  
922 stimulated with *Prevotella intermedia* lipopolysaccharide. *J Endod.*  
923 1996;22(1):9-12. Epub 1996/01/01. doi: 10.1016/s0099-2399(96)80228-7.  
924 PMID: 8618087.
- 925

**Figure 1**

*G. adiacens*



bioRxiv preprint doi: <https://doi.org/10.1101/2019.12.27.809290>; this version posted December 27, 2019. The copyright holder for this preprint (which was not certified by peer review) is the author/funder, who has granted bioRxiv a license to display the preprint in perpetuity. It is made available under aCC-BY 4.0 International license.

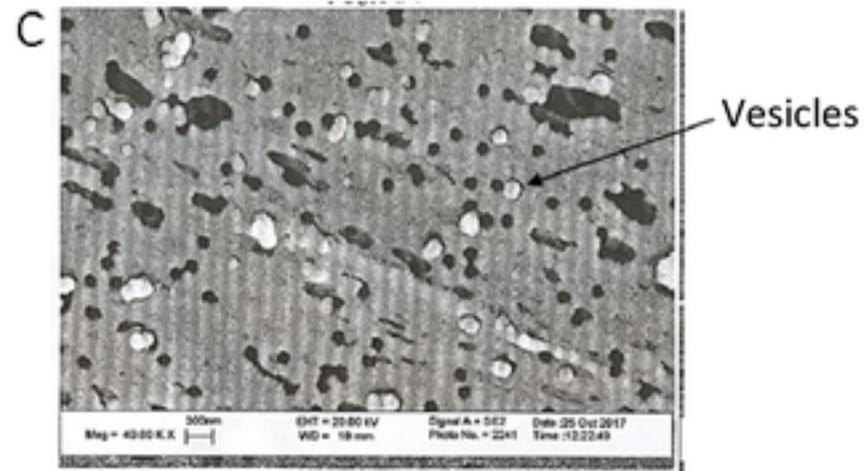


**Figure 2**

*G. elegans*

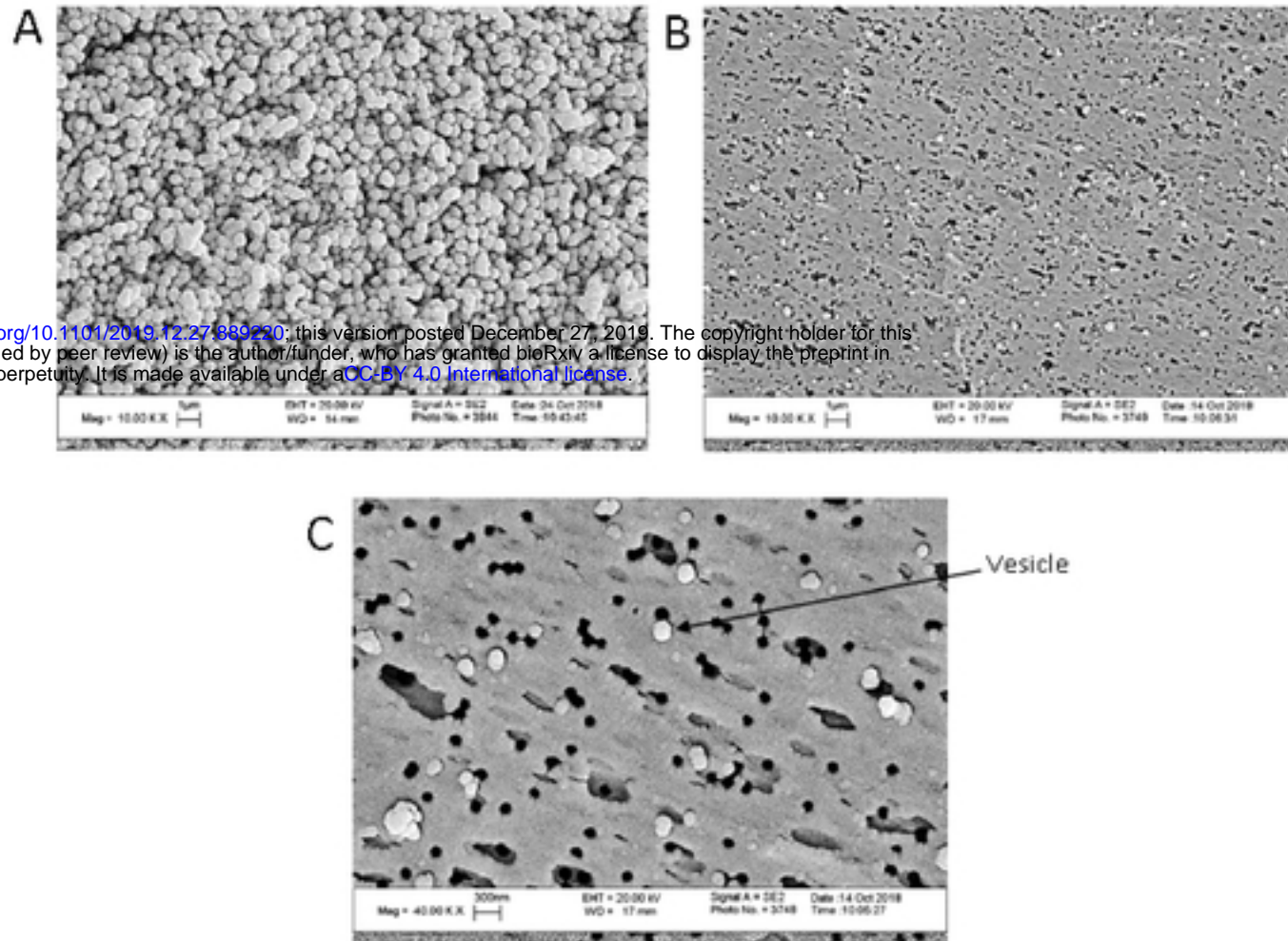




**Figure 3**

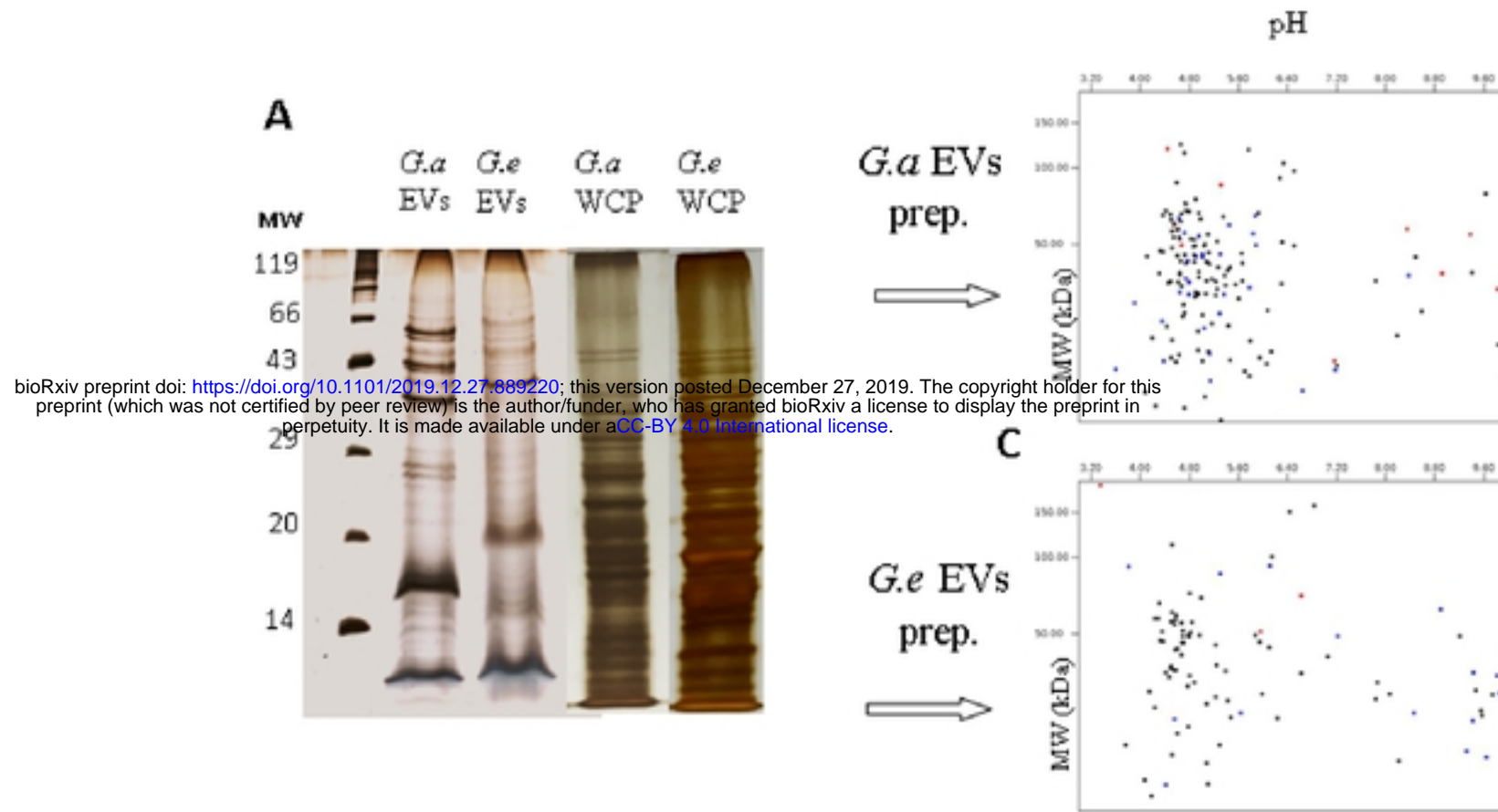


**Figure 4**

bioRxiv preprint doi: <https://doi.org/10.1101/2019.12.27.889220>; this version posted December 27, 2019. The copyright holder for this preprint (which was not certified by peer review) is the author/funder, who has granted bioRxiv a license to display the preprint in perpetuity. It is made available under aCC-BY 4.0 International license.

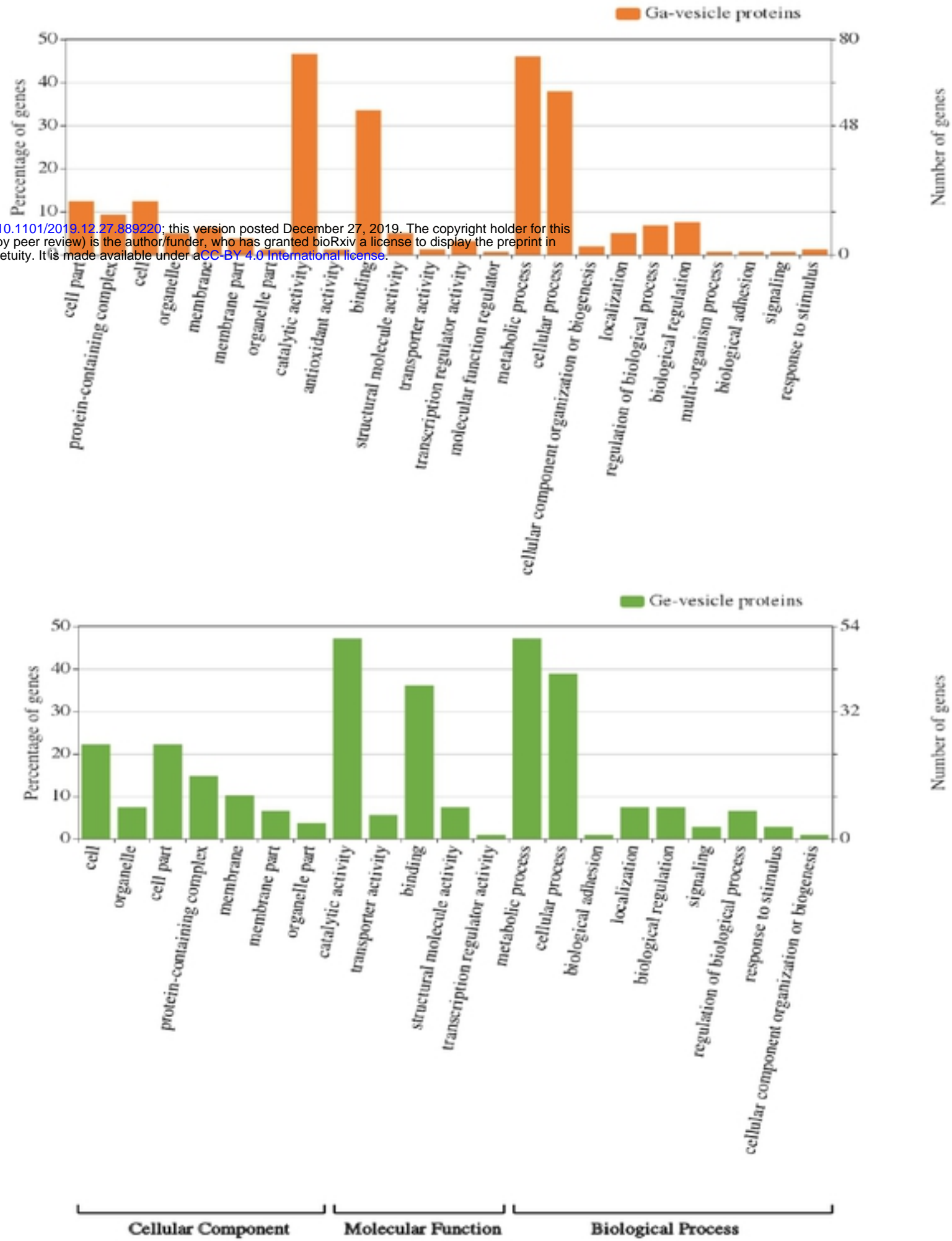


**Figure 5**

bioRxiv preprint doi: <https://doi.org/10.1101/2019.12.27.889220>; this version posted December 27, 2019. The copyright holder for this preprint (which was not certified by peer review) is the author/funder, who has granted bioRxiv a license to display the preprint in perpetuity. It is made available under a [CC-BY 4.0 International license](#).

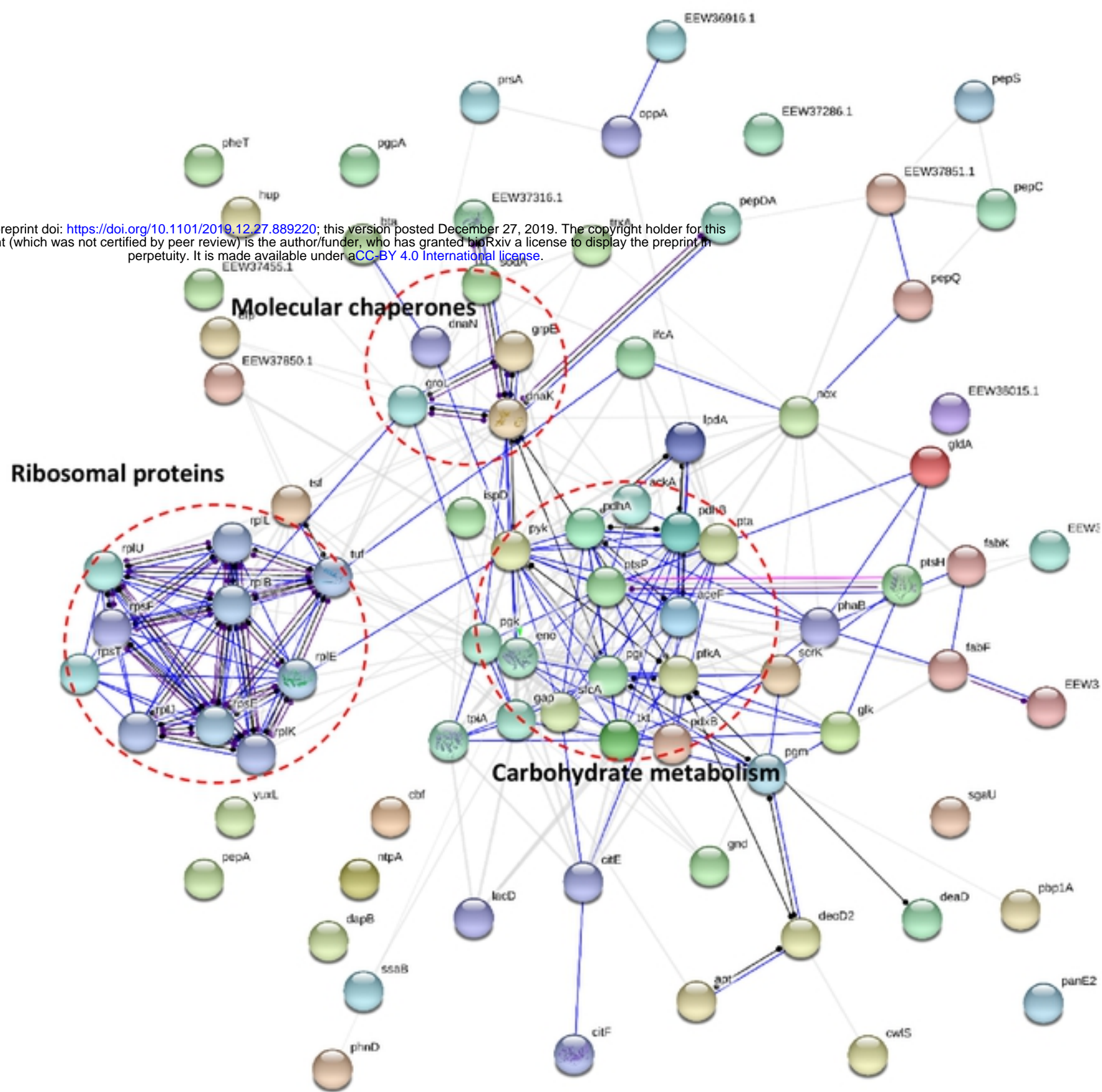




**Figure 6**

bioRxiv preprint doi: <https://doi.org/10.1101/2019.12.27.889220>; this version posted December 27, 2019. The copyright holder for this preprint (which was not certified by peer review) is the author/funder, who has granted bioRxiv a license to display the preprint in perpetuity. It is made available under aCC-BY 4.0 International license.

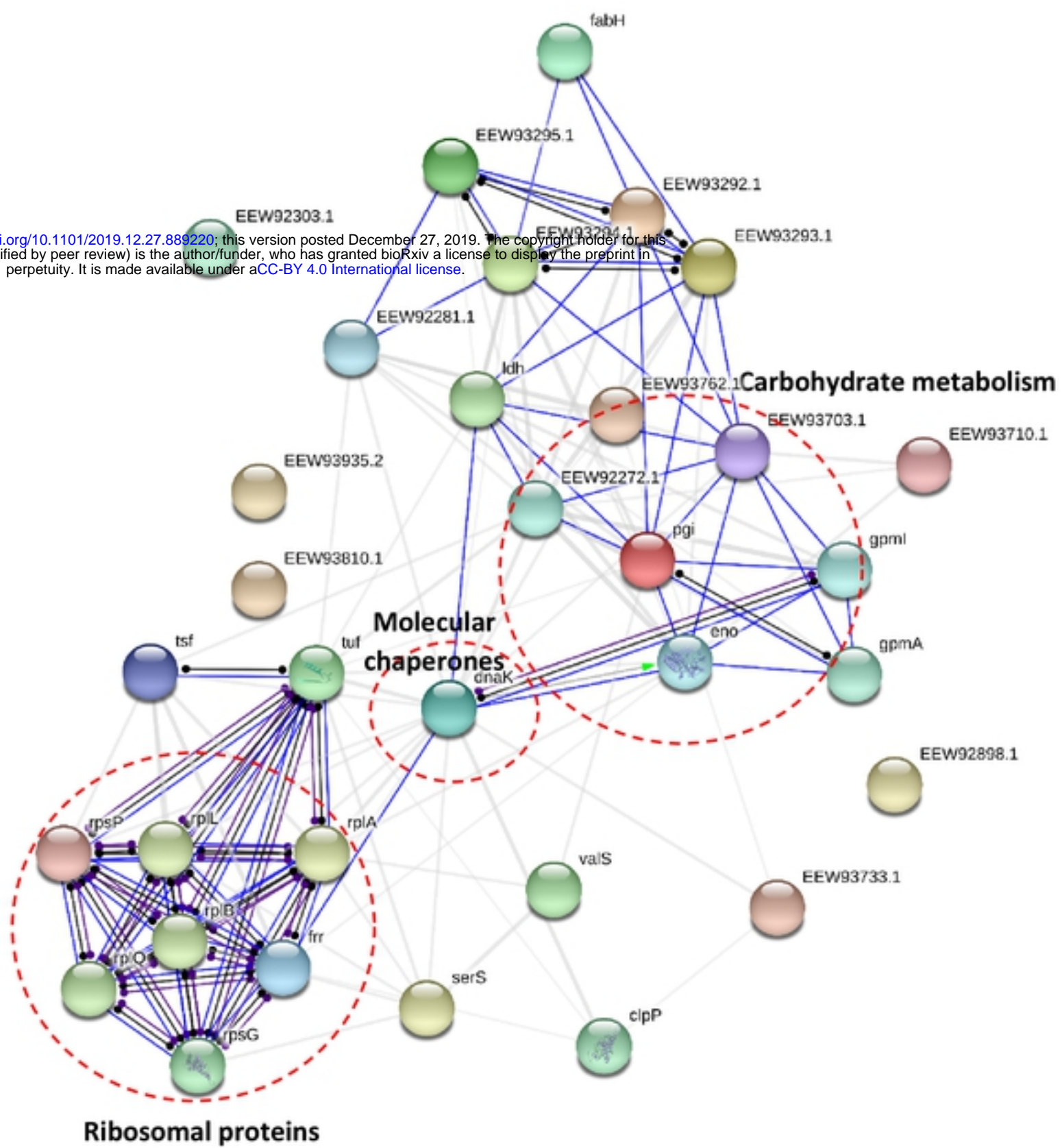
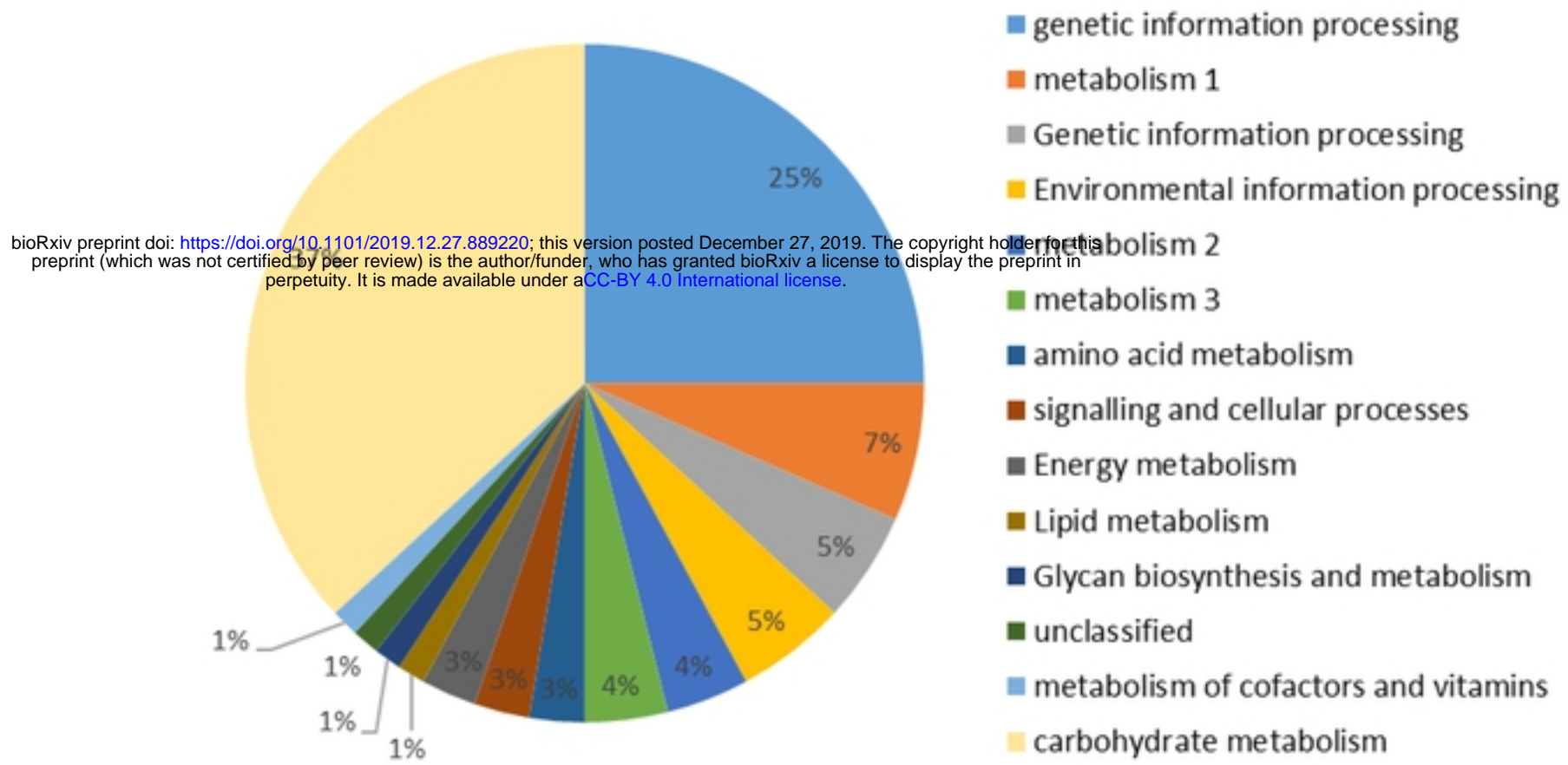


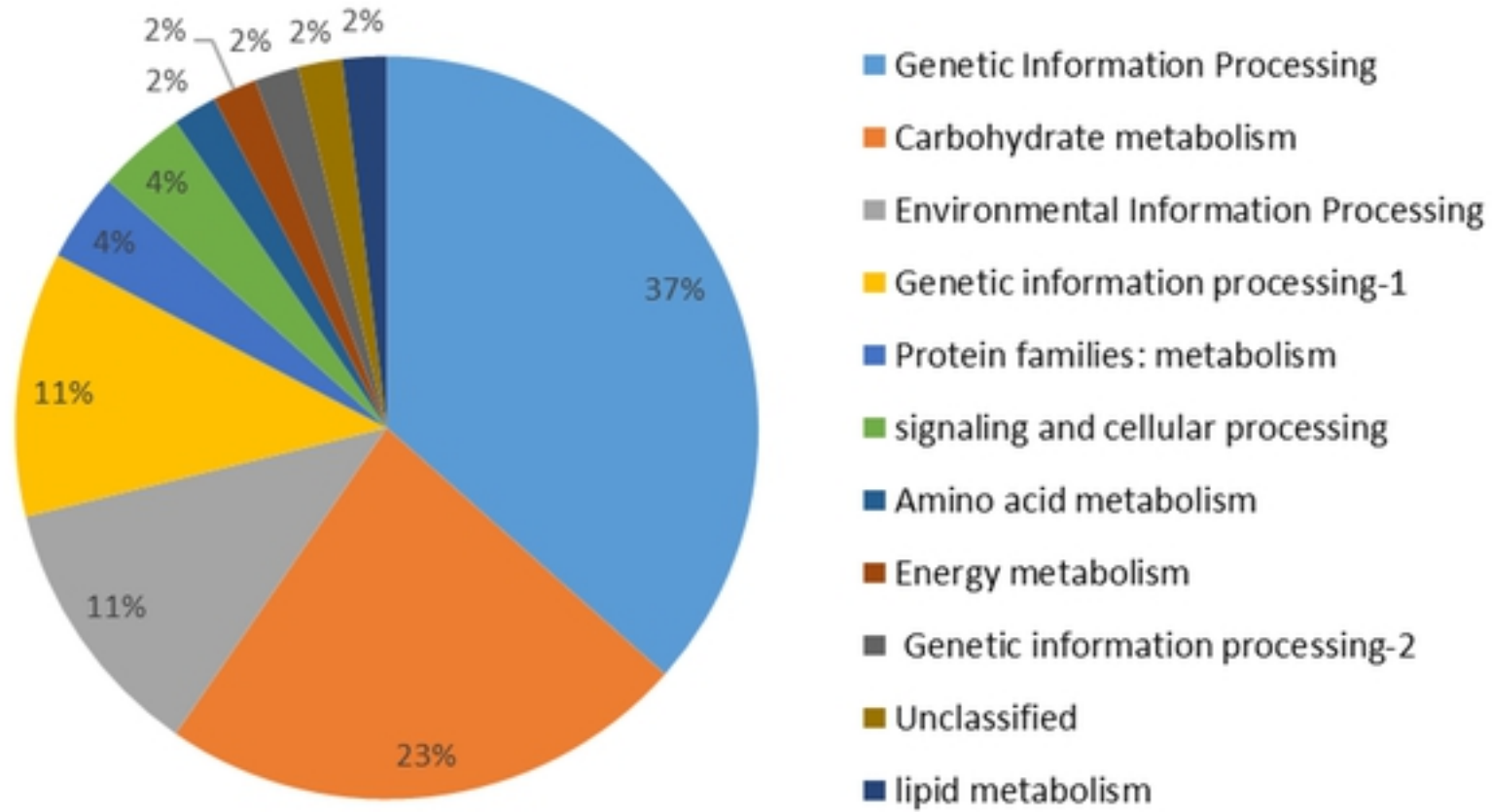


**Figure 7**

**KEGG pathways: *G. adiacens* EVs proteome**



**KEGG pathways: *G. elegans* EVs proteome**



Fig

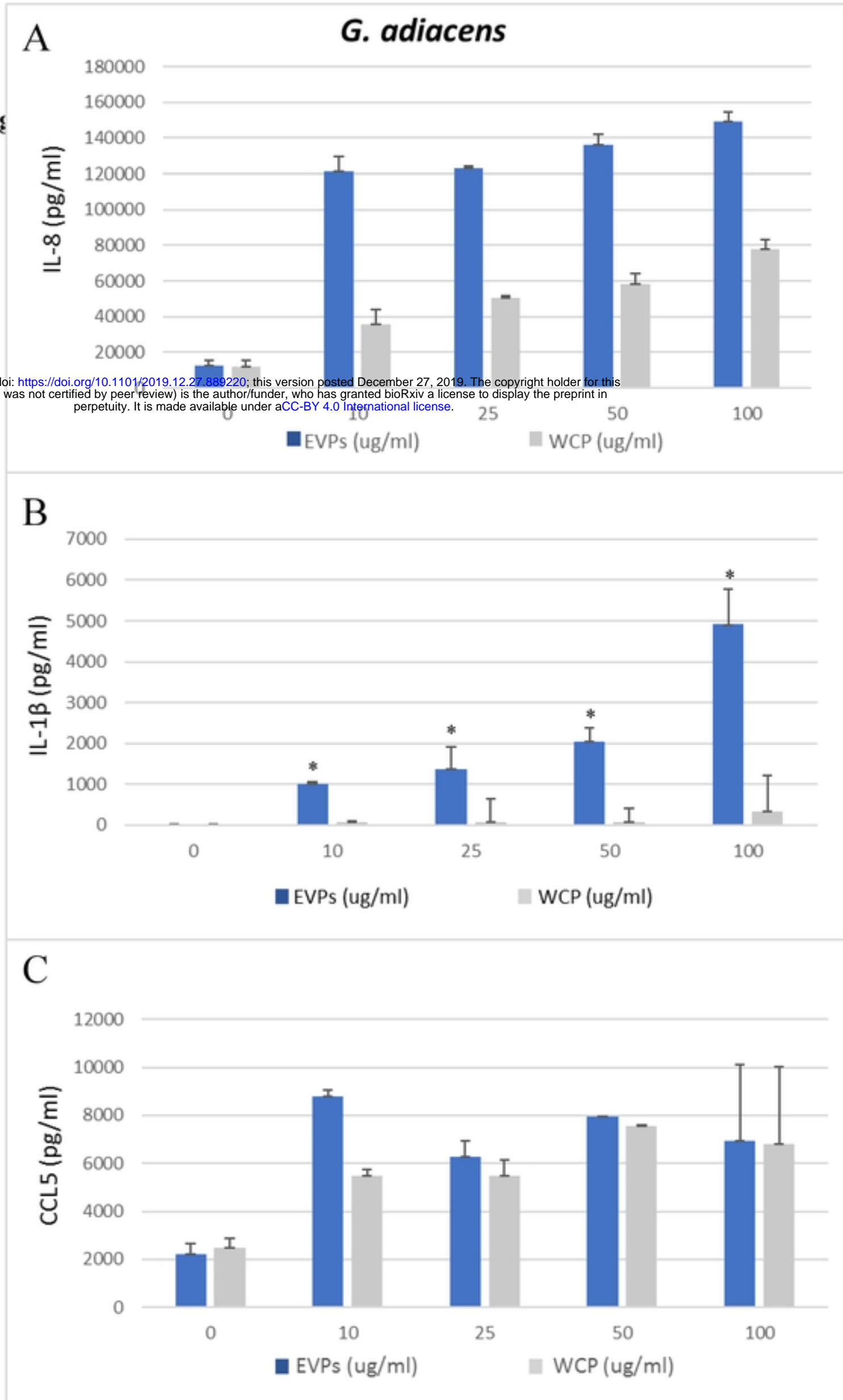


**Figure 9**

